IOWA STATE UNIVERSITY
Digital Repository

Mechanical Engineering Publications | Mechanical Engineering

9-2013

Fluid dynamics topics in bloodstain pattern analysis: Comparative review and research opportunities

Daniel Attinger
Iowa State University, attinger@iastate.edu

Craig B. Moore
Niagara Regional Police Service

Adam Donaldson
Dalhousie University

Arian Jafari
Iowa State University

Howard A. Stone
Princeton University

Follow this and additional works at: http://lib.dr.iastate.edu/me_pubs

Part of the Laboratory and Basic Science Research Commons, and the Other Mechanical Engineering Commons

The complete bibliographic information for this item can be found at http://lib.dr.iastate.edu/me_pubs/135. For information on how to cite this item, please visit http://lib.dr.iastate.edu/howtocite.html.

This Article is brought to you for free and open access by the Mechanical Engineering at Iowa State University Digital Repository. It has been accepted for inclusion in Mechanical Engineering Publications by an authorized administrator of Iowa State University Digital Repository. For more information, please contact digirep@iastate.edu.

Fluid dynamics topics in bloodstain pattern analysis: Comparative review and research opportunities

Abstract
This comparative review highlights the relationships between the disciplines of bloodstain pattern analysis (BPA) in forensics and that of fluid dynamics (FD) in the physical sciences. In both the BPA and FD communities, scientists study the motion and phase change of a liquid in contact with air, or with other liquids or solids. Five aspects of BPA related to FD are discussed: the physical forces driving the motion of blood as a fluid; the generation of the drops; their flight in the air; their impact on solid or liquid surfaces; and the production of stains. For each of these topics, the relevant literature from the BPA community and from the FD community is reviewed. Comments are provided on opportunities for joint BPA and FD research, and on the development of novel FD-based tools and methods for BPA. Also, the use of dimensionless numbers is proposed to inform BPA analyses.

Keywords
bloodstain pattern analysis, review, dimensionless number, drop generation, trajectory, impact, stain

Disciplines
Laboratory and Basic Science Research | Other Mechanical Engineering

Comments
NOTICE: this is the author's version of a work that was accepted for publication in Forensic Science International. Changes resulting from the publishing process, such as peer review, editing, corrections, structural formatting, and other quality control mechanisms may not be reflected in this document. Changes may have been made to this work since it was submitted for publication. A definitive version was subsequently published in Forensic Science International, [231, 1-3, (2013)] doi:10.1016/j.forsciint.2013.04.018.

This article is available at Iowa State University Digital Repository: http://lib.dr.iastate.edu/me_pubs/135

Elsevier Editorial System(tm) for Forensic Science International

Manuscript Draft

Manuscript Number: FSI-D-12-00913R1

Title: Fluid Dynamics Topics in Bloodstain Pattern Analysis: Comparative Review and Research Opportunities

Article Type: Review Article

Keywords: bloodstain pattern analysis, dimensionless number, review, fluid dynamics, drop generation, trajectory, impact, stain, BPA, fluid mechanics

Corresponding Author: Dr. Daniel Attinger,

Corresponding Author's Institution: Iowa State University

First Author: Daniel Attinger, Associate Professor

Order of Authors: Daniel Attinger, Associate Professor; Moore Craig, Bachelor of Science; Donaldson Adam, Assistant Professor; Arian Jafari, Master of Science; Howard A Stone, Professor

Abstract: This comparative review highlights the relationships between the disciplines of bloodstain pattern analysis (BPA) in forensics and that of fluid dynamics (FD) in the physical sciences. In both the BPA and FD communities, scientists study the motion and phase change of a liquid in contact with air, or with other liquids or solids. Five aspects of BPA related to FD are discussed: the physical forces driving the motion of blood as a fluid; the generation of the drops; their flight in the air; their impact on solid or liquid surfaces; and the production of stains. For each of these topics, the relevant literature from the BPA community and from the FD community is reviewed. Comments are provided on opportunities for joint BPA and FD research, and on the development of novel FD-based tools and methods for BPA. Also, the use of dimensionless numbers is proposed to inform BPA analyses.

Suggested Reviewers:

NOTICE: this is the author's version of a work that was accepted for publication in Forensic Science International. Changes resulting from the publishing process, such as peer review, editing, corrections, structural formatting, and other quality control mechanisms may not be reflected in this document. Changes may have been made to this work since it was submitted for publication. A definitive version was subsequently published in Forensic Science International, [231, 1-3, (2013)] doi:10.1016/j.forsciint.2013.04.018.

Acknowledgements:

The authors acknowledge financial support from Iowa State University, the US National Institute of Justice and the US National Science Foundation. Several undergraduate and graduate students at Columbia and Iowa State University have participated to the early stages of the literature review, Max Gilmore, Martin Li, Seth Aaron, Junfeng Xiao, Liqun Fu, Ashish Shah and Ying Xing. D.A. acknowledges that Herb MacDonell and then David Baldwin have introduced him to the challenges involved with BPA. D.A. is thankful to have been able to read reference [42] in his mother tongue. This solid and enlightening introduction to BPA deserves a better English translation.

Fluid Dynamics Topics in Bloodstain Pattern Analysis: Comparative Review and Research Opportunities

Daniel Attinger[a*], Craig Moore[b], Adam Donaldson[c], Arian Jafari[a] and Howard A Stone[d]

[a] Department of Mechanical Engineering, Iowa State University of Science and Technology, Ames, IA 50011, USA
[b] Niagara Regional Police Service, St. Catharines, Ontario L2R 3C6, Canada
[c] Dept. of Process Engineering & Applied Science, Dalhousie University, Halifax NS B3H 4R2, Canada
[d] Department of Mechanical and Aerospace Engineering, Princeton University, Princeton, New Jersey 08544, USA

*** corresponding author: tel +1 515 294 1692, fax: +1 515-294-3261 email Attinger@iastate.edu**

*Manuscript (without author identifiers)
Click here to view linked References

FLUID DYNAMICS TOPICS IN BLOODSTAIN PATTERN ANALYSIS: COMPARATIVE REVIEW AND RESEARCH OPPORTUNITIES 2
Abstract 2
1. Introduction 3
2. Physical forces at play in bloodstain pattern analysis (BPA) 6
2.1. Description in the BPA literature 6
2.2. Fluid dynamics description 8
3. Drop generation 20
3.1. Description in the BPA literature 20
3.2. Fluid dynamics description 21
4. Flight of drops 25
4.1. Description in the BPA literature 25
4.2. Fluid dynamics description 28
5. Impact 31
5.1. Description in the BPA literature 31
5.2. Fluid dynamics description 37
6. Staining 42
6.1. Description in the BPA literature 42
6.2. Fluid dynamics description 43
7. Synthesis of the relationship between BPA and FD concepts, summary table and opportunities 45
8. Conclusion and epilogue 51
References 52
Appendix A: Calculations of the various integrals presented in section 2.2.1 64
Appendix B: How to use of impact velocity plot in section 2.2.1, Figure 4 65

FLUID DYNAMICS TOPICS IN BLOODSTAIN PATTERN ANALYSIS: COMPARATIVE REVIEW AND RESEARCH OPPORTUNITIES

Abstract

This comparative review highlights the relationships between the disciplines of bloodstain pattern analysis (BPA) in forensics and that of fluid dynamics (FD) in the physical sciences. In both the BPA and FD communities, scientists study the motion and phase change of a liquid in contact with air, or with other liquids or solids. Five aspects of BPA related to FD are discussed: the physical forces driving the motion of blood as a fluid; the generation of the drops; their flight in the air; their impact on solid or liquid surfaces; and the production of stains. For each of these topics, the relevant literature from the BPA community and from the FD community is reviewed. Comments are provided on opportunities for joint BPA and FD research, and on the development of novel FD-based tools and methods for BPA. Also, the use of dimensionless numbers is proposed to inform BPA analyses.

Keywords: bloodstain pattern analysis, review, dimensionless number, drop generation, trajectory, impact, stain

1. Introduction

Figure 1: BPA uses FD-based methods to reconstruct a bloodletting event. In the above crime scene investigated by one of the co-authors, C.M., various bloodstain patterns are visible, namely a pool (AE), transfer stains (AB), flow patterns (AA) and several drip stains (AD). Elliptical bloodstains (B) indicate the area of origin of a blood spatter, see section 5. For a description of what happened in the photographed crime scene, refer to section 8.

While the disciplines of bloodstain pattern analysis (BPA) in forensics and that of fluid dynamics (FD) each have a rich history [1, 2], interactions between these communities have not always been strong. From its infancy in 19th century Germany, BPA has aimed for practical answers to specific questions of the kind: "How did the bloodletting event of Figure 1 happen?" FD was born in the 17th and 18th centuries, in England, Switzerland and France. In contrast to BPA, FD aims to quantitatively describe the motion of fluids (gases or liquids), and the causes of the motion, with general equations. FD typically defines the initial and boundary conditions of a fluid system, and from there describes how the system evolves in time and space, most often in a *deterministic* manner. BPA typically solves the indirect problem of inspecting stains in a crime scene to infer the *most probable* bloodletting event that produced these patterns. In both the BPA and FD communities, scientists study the motion and phase change of a liquid in contact with air, or with other liquids or solids. The need for better integrating FD and BPA is mentioned in a 2009 report [3] by the US National Research Council, entitled "Strengthening Forensic Science

in the United States: A Path Forward". The report mentions that "the uncertainties associated with bloodstain pattern analysis are enormous", states that a minimum requirement to make BPA interpretations is to have "an understanding of the physics of fluid transfer", and advocates for stronger scientific foundations for BPA, given "the complex nature of fluid dynamics". It is also our conviction that the FD and BPA communities could benefit from a deeper understanding of each other. Specifically, by following the path proposed by the US National Academies, BPA can obtain new quantitative tools and methods, while FD may be presented with new flow problems.

Note that there are two overlapping communities in BPA: the users and the researchers. BPA researchers, the specific target of this review, evaluate existing BPA techniques for accuracy, for example; they also develop new BPA techniques. Their research is typically funded by Governmental Agencies, run in Government laboratories or in universities and published in journals such as Forensic Science International or the Journal of Forensic Sciences of the AAFS (American Academy of Forensic Sciences).Users of BPA techniques study specific crime scenes, funded by the Police Administration or hired as trial consultants. Articles with direct practical relevance, targeting users, are typically published by the International Association for Bloodstain Pattern Analysis (IABPA) Journal or the Journal of Forensic Identification of the International Association for Identification (IAI). It is also our conviction that a better integration of FD and BPA will provide better, maybe simpler tools for BPA users. Also, some of the ideas of the manuscript may be useful to instructors for either identifying science topics useful for education of future practitioners or for contributing to the continual education of practitioners interested in introducing more scientific approaches into their work.

This review is organized in five parts. First, section 2 describes the *physical forces* driving the dynamics –the motion and its causes- of blood as a fluid. Then, the formation of bloodstains is described as a deterministic sequence of events, in separate sections on *(3) drop generation, (4) drop trajectories, (5) drop impact, and (6) stain formation*.

For each of the five topics listed above, a summary and comparative review of relevant literature is presented, first the BPA literature, and then the FD literature. The purpose of this manuscript

is to describe the FD themes and research topics that affect BPA. It is not intended to be a review of each individual field, but a comparative review of the overlapping areas to facilitate identification of potential inter-community collaborations. For instance, a synthesis of the connections between FD and BPA is proposed in section 7, describing how well the problems are understood and what opportunities exist for new research and the development of novel tools and methods. The findings of our review paper are then summarized in Table 4, which highlights the relations between BPA terminology (rows of the table) and FD concepts (columns). It is our hope that this manuscript will be used to assess the state-of-the-art and to identify untapped research topics at the intersections of FD and BPA.

2. Physical forces at play in bloodstain pattern analysis (BPA)

2.1. Description in the BPA literature

Several classic BPA textbooks [1 , 4, 5] include a comprehensive section on the biological and physical properties of blood, describing this complex fluid and its main physical properties, such as density, viscosity and surface tension. Typical values of these properties are provided in Table 1. Generally defined, blood is an aqueous liquid, with about half of its volume consisting of micrometer-size particles such as red and white blood cells. An indicator of the concentration of particles in the blood is the hematocrit, which is the measurement of the relative volume of red blood cells versus the total blood volume [1]. The density of blood, its mass per volume, 1060 kg/m^3, is close to that of water. The same textbooks also describe how the porosity, roughness and wettability of a blood-stained surface, called target surface, influences the observed stains. Viscosity is typically presented as a measure of the resistance of a fluid to a change of shape or flow [5]. The viscosity of blood at body temperature is reported as approximately four times larger than that of water [5]; the viscosity of blood decreases with increasing temperature [5] and increases with increasing hematocrit [6]. Blood is also described as non-Newtonian fluid, i.e. a fluid with a viscosity that varies with the flow conditions [5].

Surface tension, also referred to as the surface energy, is the measure of the energy to change the interfacial area between two immiscible fluids, here blood and air. Surface tension plays a key role in the generation of drops and their impact on surfaces. Surface tension decreases with increasing temperature and is affected by chemicals present within the blood [7].

Often, BPA work reports measurements of velocities, drop sizes or stain sizes corresponding to a specific experiment [8, 9], without attempt to generalize the conclusions to other experimental conditions. Sometimes empirical correlations are fitted to a set of BPA data [10-12] with little consideration for the physical basis of these correlations, or for their domain of validity. These approaches might induce conceptual errors and, possibly could be replaced by a physical and dimensionless description, as in [13, 14], to compare the relative importance of the physical forces. These ideas are discussed in more details below.

Blood Properties	**Human Blood**	**Animal Blood** (species dependent)	**Distilled Water**	**Sources, Control Factors and Notes**
viscosity, μ ($\times 10^{-3}$ kg/ms)	20°C: 6..3 37°C: 4.4 (1.6 – 5.1)	20°C: 8.6 37°C: 5.5 (3 – 20)	20°C: 1.0 37°C: 0.7	[1, 4, 7, 15-18] *Temperature, shear rate, hematocrit*
surface tension between air and blood, σ ($\times 10^{-2}$ N/m)	20°C: 6.1 37°C: 5.2 (2.7 – 5.8)	20°C: 6.5 37°C: 5.1	37°C: 7.0 20°C:7.3	[1, 4, 7, 19, 20] *Temperature, shear rate, hematocrit*
density, ρ (kg/m^3)	1060 (1052 – 1063)	1062	993	[4, 19] Values at 37°C
hematocrit, *H*	0.40 (0.40 – 0.45)	0.4 (0.39 – 0.46)	0	[1, 4, 19]

Target Properties	**Range of Values**	**Control Factors and Notes**
surface roughness, *Ra* (m)	1×10^{-10} – 1×10^{-2}	Dependent on material, its manufacturing process and surface preparation
wetting Angle, θ (degrees)	0 (very clean glass) – 140 (waxed car)	Dependent on material, its manufacturing process and surface chemistry
elasticity, *E* (x 10^9 Pa)	0.001 (rubber) – 1000(diamond)	Dependent on material
permeability, *k* (m^2)	1×10^{-7} (gravel) – 1×10^{-19} (granite)	Dependent on material and internal microstructure, can be predicted with the Kozeny−Carman model. [21]
porosity, ϕ (m^3 void/m^3 material)	0 – 0.4	Dependent on material and internal microstructure

Impact and drying scales	**Range of Values**	**Control Factors and Notes**
velocity, *v* (m/s)	0 – 100	Low velocities typical of free-falling droplets; high velocities typical of gunshot scenarios.
diameter, *d* ($\times 10^{-3}$ m)	1×10^{-3} (1μm) – 5 (5mm)	Smaller drops are typically released in high-energy, high-velocity situations.
shear rate γ, (1/s)	0 – 20000	The larger shear rate corresponds to the impact at 100m/s of a 5mm drop on a target.
volume, *V* ($\times 10^{-9}$ m^3)	5.2×10^{-10} (0.5 femtoliter, fL) – 65 (65μL)	Volume of a blood drop
mass, *m* ($\times 10^{-6}$ kg)	6×10^{-10} (0.6 picogram, pg) – 69 (69 mg)	Mass of a blood drop

Table 1: Physical properties and parameters relevant to the FD of BPA, with controlling factors. Typical values are given, while the intervals in parenthesis correspond to the published range of value.

2.2. Fluid dynamics description

In FD, a fluid is characterized in contrast to a solid, and with respect to some physical properties. What defines a liquid versus a solid is the deformation in response to stresses like shear or elongation: solids respond to stresses by a sudden deformation, until a new equilibrium configuration is reached, while fluids continually deform as long as a shear stress is applied. Within FD, the viscosity is defined as the ratio between applied stress and the rate of fluid deformation: the higher the viscosity, the higher the stresses needed for the same fluid deformation (or flow). Viscosity dissipates the energy associated with the deformation of a fluid. In relation to BPA, viscosity dampens the shape oscillations of drops in flight and resists the spreading during impact. The viscosity of liquids typically decreases with increasing temperature.

For complex liquids such as blood, which contain suspended particles, the viscosity changes with the shear rate (see Table 1 for values of shear rates representative of BPA). Such a fluid with a non-constant relation between stress and rate of deformation is called *non-Newtonian.* Blood is further classified as shear-thinning, a specific class of non-Newtonian fluids for which viscosity decreases with increased shear. Indeed, blood appears more viscous when it drips from a wound than when it impacts a target at several meter/second. The viscosity of the blood also increases with increasing hematocrit and decreasing temperature. The viscosity μ of blood can be modeled from experiments in the form [16] of $\mu=\mu_{ref}\cdot g(H)\cdot f(\gamma)\cdot k(T)$, where μ_{ref} is the viscosity at a reference level of temperature (typically 37°C); and the respective functions g, f and k model the dependence of the viscosity on hematocrit, shear rate and temperature, respectively. Other models do exist, such as that given in [22], to describe the measured viscosity of human blood for shear rates from 2/s to 100,000/s.

Surface tension is a force over a length, or an energy per unit area, that characterize any interface between two materials of different physico-chemical structure, such as blood and air. Surface tension affects the drop formation process, the breakup of jets [23] and the oscillations of the shapes of drops. Surface tension tends to keep the drops spherical in flight since spherical shapes minimize the surface energy [24]. This tendency of drops to assume a spherical shape is

important to BPA, especially in relation with the determination of impact angles from the ellipticity of stains.

Regarding the target substrate, the important physical properties are the elasticity, permeability, porosity, roughness and wetting angle. The elasticity *E* of a target is the ratio of the applied normal force per area to the resulting relative deformation of the solid surface, called the strain. For example, microscopic deformations of a rubber target during drop impact have been shown to influence the splashing of the drop [25]. The permeability is related to the ability of a liquid to flow through a porous target. The porosity is a measure of the typical pore space available for a fluid [21]. The roughness is a representative measurement of the departure of the surface texture from an absolute flatness; it is commonly expressed as *Ra*, the arithmetic average of that departure. The wettability describes how a solid target influences the motion of a pair of immiscible fluids along it [26], for example water/air or water/oil. In BPA, wettability influences the stain size and their drying. In the case of BPA, the system of interest involves the two fluids of blood and air, as well as a solid target. The wettability of a system is illustrated in Figure 2, and depends on the system chemistry, physical state (cold or hot) and target microstructure or roughness. It is characterized by the wetting angle measured at the edge (also called the wetting or contact line) of a small drop on top of the target, referred to as the static wetting angle. A small wetting angle ($\theta \sim 0^o$) corresponds to a hydrophilic state, while a large wetting angle ($\theta > 120^o$) correspond to a hydrophobic state, as the liquid tends to be repelled from the substrate. Note that the wetting angle dynamically adjusts its value when the wetting line moves, for example during impact or evaporation [27].

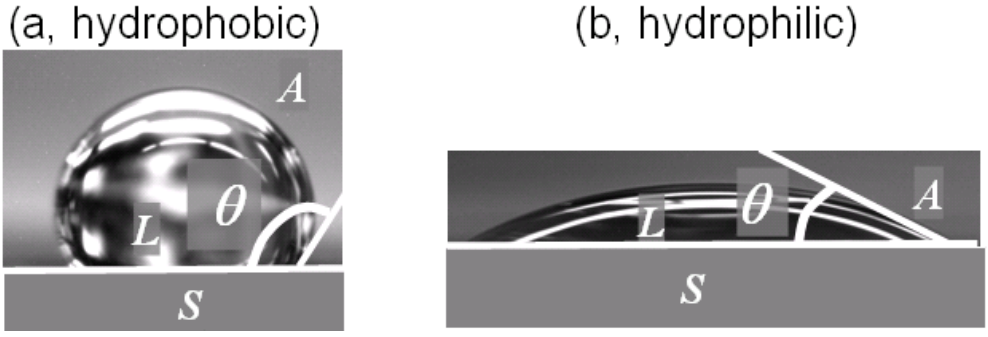

Figure 2: Wetting angle θ on a hydrophobic target (*a*, such as an oily, plastic or waxed surface) and on a hydrophilic target (b, such as clean glass). The wetting angle is measured at the three-phase line, which is the location where the air (A), the liquid (L) and the solid (S) meet. Drop impact and stain formation depend on wettability.

2.2.1. Dimensionless numbers

The same discipline of FD describes the motion of gases in extra-terrestrial space [28], the dynamics of atmospheres and oceans, and the motion of blood in capillaries thinner than a human hair [29]. To describe within a single framework events that span such a large range of time and length scales, FD relies on a three step analysis: first, the magnitude of all the forces acting on the fluid are evaluated, as in Table 2; then the relative magnitude of pairs of these forces is compared using scaling or dimensionless numbers, such as the ones listed in Table 2, for example the Reynolds or Weber number; finally a more detailed analysis is performed based only on the most relevant forces, neglecting those that are comparatively negligible. FD methods for detailed analysis include various analytical methods (solving FD equations with pen and paper), numerical methods (solving FD equations with a computer), or experimental methods (for example high-speed visualization). On one hand, detailed FD analyses provide accurate solutions, but can be cumbersome and mathematically challenging. On the other hand, proper use of dimensionless numbers result in simpler analyses valid for a wide range of experimental conditions, allowing experimental outcomes (stain dimension, number of spines, splashing versus no splashing) to be inferred for cases that have not been (*or can not be*) tested explicitly. In other words, the fluid dynamicist knows that two liquids behave similarly as long as they are in the same physical regime, i.e. as long as they are experiencing the same ratios of forces. Therefore, what influences BPA events is not so much the physical properties of the blood, air and target, or the velocities of the bloodletting event, but rather the balance between the forces at play, expressed with dimensionless numbers. Indeed, these Reynolds and Weber numbers are not a way to express practical data (such as velocities or length) in a more complicated way, but they help answer practical questions. Sections a-c below illustrate the importance of dimensionless numbers with the elementary BPA problem of determining the impact velocity v of a drop with diameter d moving downwards towards a target.

Force	Physical Expression	Magnitude in BPA, in N (Newton)	Physical Meaning
inertial forces	$\rho v^2 d^2$	0 to 265	mass × maximum possible acceleration of a moving volume of fluid, i.e. a drop
capillary forces	$\sigma d \cos\theta$	-4 to 5	force due to surface tension, parallel to the interface between two fluids, acting on the 3-phase line (see Figure 2)
viscous forces	$\mu v d$	0 to 2×10^{-3}	Dissipative forces due to friction in a moving fluid
gravity force	$\rho g d^3$	0 to 0.001	Attractive force acting on a volume of fluid, directed towards the center of the earth
Dimensionless number	**Definition**	**Magnitude in BPA**	**Ratio of Forces**
Reynolds number	$Re=\rho v d/\mu$	0 to 100,000	Inertia to viscous forces, describes the drag during the flight of a drop and the impact of a drop on a surface
Weber number	$We= \rho v^2 d/\sigma$	0 to 1×10^7	Inertia to surface forces, describes jetting, impact and drop oscillations
Capillary number	$Ca= \mu v /\sigma$	0-8	Viscous to surface forces, describes wetting and imbibition
Bond number	$Bo=\rho d^2 g/\sigma$	0-5	Gravity to surface forces, controls spreading of large drops or streams; establishes the shapes of static drops
Froude number	$Fr=v^2/dg$	0 to 1×10^{12}	Inertia to gravity, controls spreading and flight of drops
Drag coefficient	$C_D= F_D/½\rho_a v^2 A_d$	0.3 to 1×10^5	Ratio of the drag force to the stagnation pressure force caused by the motion of the drop in air

Table 2: Forces and typical dimensionless parameters used to describe FD phenomena, with typical magnitudes in BPA cases.

(a) a dimensionless curve replaces multiple dimensional curves: Let us start with the simplest experiments where a drop from a dropper drips towards the ground. Let us control the height *h* of the fall and measure the duration *t* of the fall with a chronometer or with a high-speed camera. Like Galileo [30, 31], we find, at least for moderate heights, that *h* is proportional to t^2 , i.e. *h (in meter, noted m)* $\cong$ t^2*(in second square, noted* s^2*).* Using together the measured values of *h* and *t,* and the physical principle that a valid equation needs to have the same units on both sides of the equal sign, we find the equation for the travel of the drop as $h = ½gt^2$, where we have identified in *g* the gravity constant with units of, necessarily, m/s^2. We might then realize that a drop that falls from higher than one meter typically takes more time than predicted by the equation $h = ½gt^2$. The culprit for slowing down the drop is the drag, the resistance force exerted by the air on the moving drop. Figure 3a shows values of the drag force on spherical drops moving through air, as a function of their velocities and diameters. The drops have various diameters, representative of BPA situations. For low velocities and small drops, the relation is a straight line because the drag force is proportional to *v*; for larger and faster drops, the relation becomes a parabolic line

indicating that drag forces become proportional to v^2. The transition between these two behaviors (a proportion to v and then to v^2) occurs at different velocities for different droplet sizes.

In contrast, Figure 3b describes the same relationship between drag and velocity in a dimensionless way, and all the results of Figure 3a collapse along a single curve. To do so, the drag force is reported as the drag coefficient (C_D, defined as in equation (2) below) and plotted against the Reynolds number (defined in Table 2). The information conveyed with the dimensionless plot in Figure 3b is the very same as in the dimensional plot of Figure 3a, except that one dimensionless curve replaces several dimensional curves.

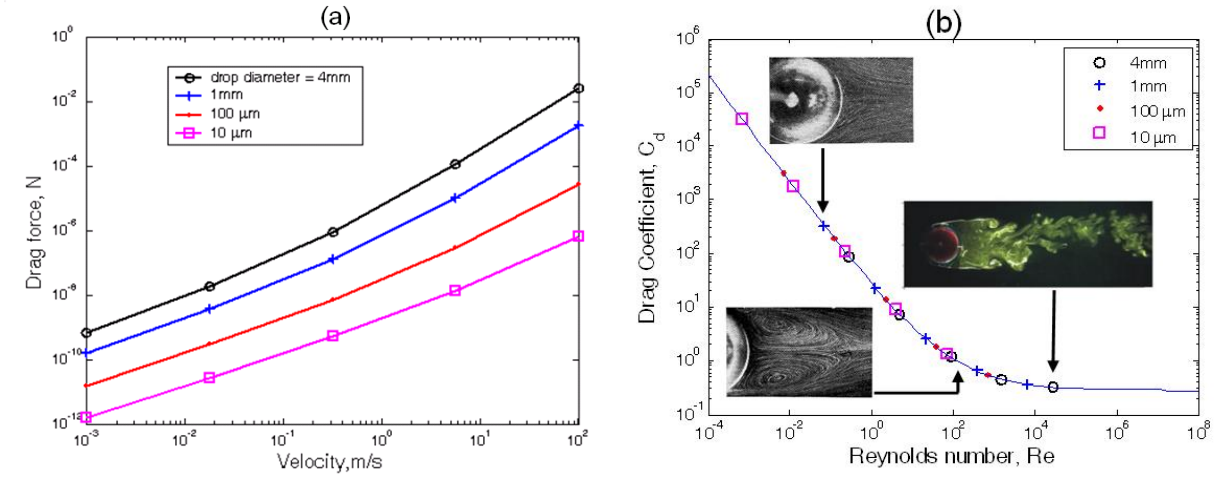

Figure 3: Determination of the drag force as a function of the velocity of a drop moving through quiet air. Dimensional plot (a) versus non-dimensional plot (b). Note that in (b) all the datapoints collapse onto the single line of Eq. (3) when reported using dimensionless numbers. In the photographs, the general flow direction is from left to right, and particles added to the fluid (from [32, 33], with permission from publisher) follow the fluid flow around a sphere.

(b) a dimensionless plot tells more about the physics at play than multiple dimensional plots: In the dimensionless plot of Figure 3, the transition between a linear and parabolic relationship between the drag coefficient and the velocity v corresponds to the transition between the region where C_D decreases with Re, and the region where C_D is constant with Re. This transition occurs over a well determined range of Reynolds number, corresponding to a change of physical regime, i.e. a change in the respective importance of inertial and viscous forces (Table 2): at low Re the flow is steady and drag is mostly caused by friction forces, corresponding to a linear dependence between C_D and Re, while at Re higher than ~100 turbulence and unsteadiness develop, as exemplified by the pictures of the flow at $Re>10^4$. This

chaotic motion of the air around the droplet corresponds to inertial forces being the main cause of the drag, overcoming viscous forces, and results in a parabolic relationship between C_D and *Re. The ability to see the transitions between dominant forces comes with the use of dimensionless numbers in FD.*

An illustrative example of the advantages *a* and *b* of using dimensionless numbers in BPA is provided by the impact velocity map elaborated in Figure 4. This map provides the impact velocity (expressed by the contours of ratios of impact velocity to terminal velocity) of a drop striking a target, as a function of the initial release conditions (i.e. initial drop diameter d_0 and initial velocity v_0). For simplicity in Figure 4, v_0 is oriented downwards, and the target is placed horizontally, one meter below the release location. The initial conditions in Figure 4 are representative of various conditions encountered in BPA, with $10^{-3}\,mm \le d_0 \le 5\,mm$ and $0.1\,m/s \le v_0 \le 240\,m/s$.

In this situation of a drop flying towards a target, only two forces are active: the weight of the drop, and the drag between the blood and surrounding air. The motion of the droplet towards its target can be accurately computed, considering how these two forces affect its initial velocity and position during the flight. Mathematically, this motion is described by Newton's second law

$$m_d \frac{d\vec{v}}{dt} = m_d \vec{g} - \vec{F}_D \ , \tag{1}$$

where $m_d, \frac{d\vec{v}}{dt}, \vec{g}$ and $\vec{F}_D$ are the droplet mass, droplet acceleration, gravitational acceleration and drag force, respectively. The above equation simply means that during the time of its flight, the velocity of the droplet is modified by two forces, its weight and the drag.

The value of the drag force is expressed with the correlation

$$\vec{F}_D = \rho_a C_D \frac{A_d}{2} \vec{v} v \ , \tag{2}$$

where ρ_a, A_d, v and $\vec{v}$ are the air density, the cross-sectional area of the droplet, the velocity magnitude and velocity vector of the droplet. The dimensionless parameter C_D is the drag

coefficient plotted in Figure 3b. For BPA cases, C_D is best expressed by the correlation of Lavernia et al. [34], valid for $0.1 \le \mathrm{Re} \le 4000$:

$$C_D = 0.28 + \frac{6}{\mathrm{Re}^{0.5}} + \frac{21}{\mathrm{Re}}, \qquad 0.1 \le \mathrm{Re} \le 4000. \tag{3}$$

Figure 3b shows how C_D varies with the Reynolds number $Re=\rho_a v d/\mu_a$, where μ_a, v and d are the density and dynamic viscosity of the air, and the droplet velocity and diameter, respectively. The impact velocities and terminal velocities in Figure 4 have been integrated with respect to time using equation (1), with an explicit discretization method that was tested for convergence.

In a plot such as Figure 4, non-dimensional numbers are used in many ways: first the initial velocities (vertical axis) and impact velocities (contours) are displayed as ratios relative to the terminal velocity. This allows the presentation of a wide range of velocities in the same plot, more accurately than if velocities were plotted dimensionally. Also, the different physical regimes are best identified with dimensionless numbers and correspond to specific regions indicated by squared numerals in Figure 4. Let us show now how these different physical regimes are related the following questions, fundamental for BPA studies.

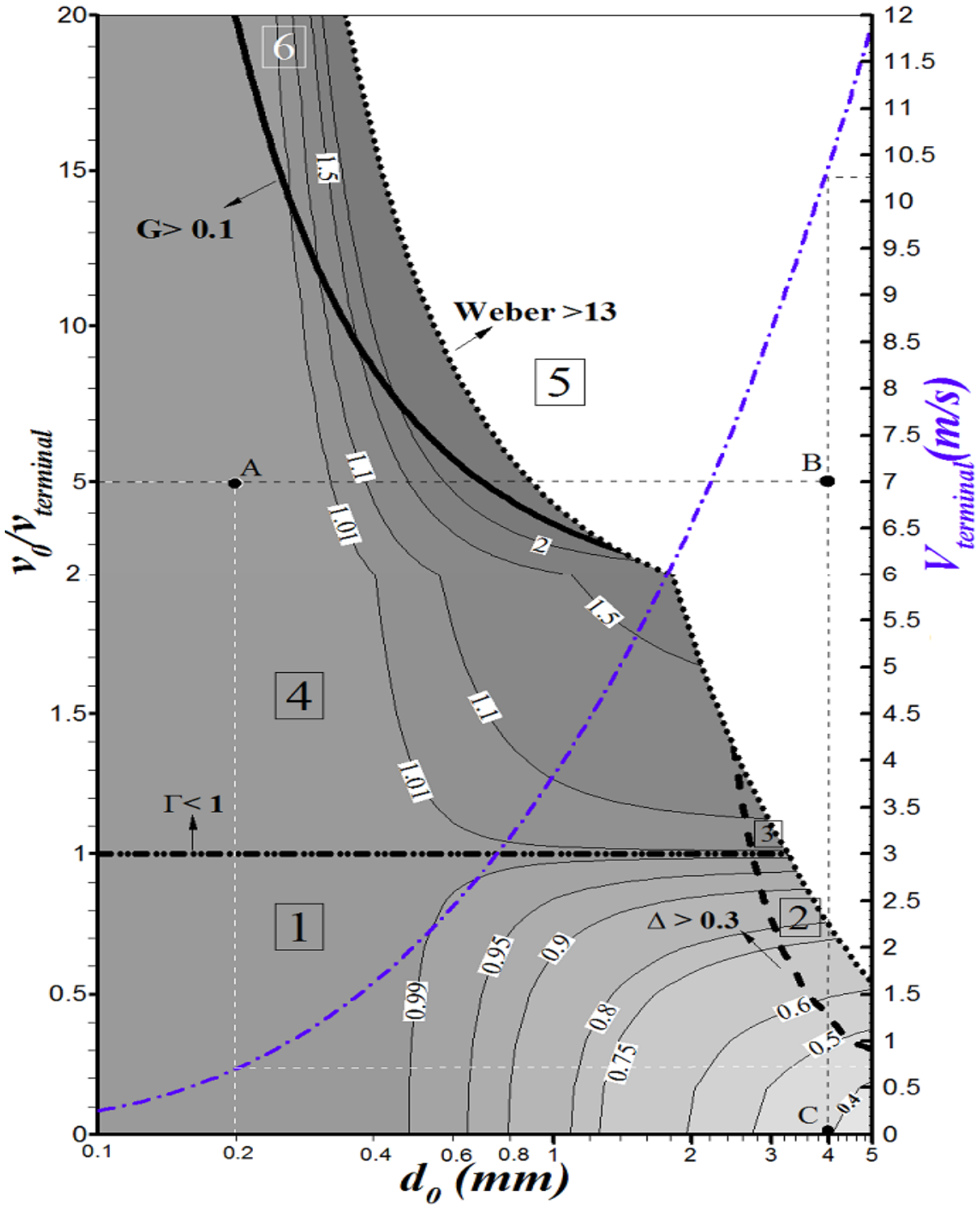

Figure 4: Semi-dimensionless plot to determine the impact velocity of a falling droplet as a function of droplet diameter, d_0, and initial droplet velocity, v_0, for a vertical path (trajectory) of 1m. The initial velocity points downwards. Note that both axes are non-linear to better display the data, and that detailed instructions to use the plot are in Appendix B. Both the impact velocity (thin contours in the body of the plot) and the initial velocity are given in a non-dimensional manner, as ratios over the terminal velocity. The terminal velocity $v_{terminal}$ is the violet curve, with values on the vertical axis, right. The thick lines delineate various physical regimes, identified with squared numerals and described in Table 3 and point *b* below.

b1. Will the drop break into smaller drops? In flight, breakup occurs when aerodynamic forces, i.e. the drag of the air on the droplet, overcome the surface forces at the droplet-air interface. In-flight breakup is important to the reconstruction of trajectories. The larger the drop and the higher the velocity, the higher the chances that the drop breaks up during its flight. To evaluate the possibility of breakup more rigorously, the aerodynamic drag force is compared with the surface force [35]. This comparison is expressed with the dimensionless Weber number,

$$We = \frac{\rho_a v^2 d}{\sigma} \quad , \tag{4}$$

where ρ_a, v, d, and σ are the density of air, maximum velocity, droplet diameter, and surface tension, respectively. Should *We* be significantly smaller than *1*, the droplet travels without breaking up, because surface forces win over drag forces. Should *We* be on the order of *1*, the droplet will significantly deform. At even larger *We*, the deformation becomes so severe that the drop disintegrates into smaller ones, because drag forces win over surface forces. While the reasoning above is based on a dimensionless FD number, experiments are needed to determine the exact value of the Weber number above which drop breaks up. As shown in [36, 37], breakup typically occurs for *We>13*, i.e. in the region above the thick dotted line in Figure 4, plotted for values of *We=13* based on the initial drop diameter and velocity. As a result, no impact velocities are provided in that region, because the formalism exposed here cannot predict how in-flight break-up affects the trajectory.

b2. Will gravity forces significantly modify the initial velocity?

The question of the influence of the gravitational force on the trajectories is important in BPA. If acceleration due to gravity is negligible during the droplet's flight, there is no need to consider curved trajectories. Gravity forces act all along the trajectory, but do they significantly modify the trajectory? For the specific case in Figure 4, gravity will significantly modify the initial velocity if the work of the gravity along the droplet path, W_g, is significant with respect to the initial kinetic energy of the drop E_{k0}. This comparison is expressed as the dimensionless number

$$G = \frac{W_g}{E_{k0}}, \tag{5}$$

and shown in Figure 4, where a thick solid line delineates the region G>0.1. To the left of that line, gravity forces will modify the initial velocity significantly, while to the right of that line, gravity forces will not modify significantly the initial velocity. An exact expression of G is given in Appendix A.

b3. Will the drag force significantly affect the trajectory?

The question of the influence of the drag force on the trajectories is important in BPA. If drag is negligible, then ballistic trajectories can be calculated without accounting for the drag force – which are a complicated function of the drop velocity, see Eq. (3).

In layman's terms, the question of interest is "Will the drag forces slow down the drop a lot or just a little bit?" To answer that question in FD terms, the work W_D of the drag forces along the entire trajectory needs to be compared with the initial kinetic energy of the drop, E_{k0}.
This comparison is expressed by the dimensionless number

$$\Delta = W_D / E_{k0}\,. \tag{6}$$

Should Δ be significant, for example $\Delta > 0.1$, then the work of drag forces will modify the initial velocity significantly. Should Δ be negligible, for example smaller than approximately 0.1, then the drag forces will not modify significantly the initial velocity along the trajectory. For example, if a cloud of drops is produced with a given velocity, the larger drops typically travel further away from the region of origin, because their Δ value is smaller than that of the smaller drops. This phenomenon explains why for example in gunshot spatters the small stains are found closer to the area of origin.

Due to the change in velocity along the droplet's path, both W_D and Δ need to be calculated numerically (with a computer, according to the full definition of Δ in Appendix A). In Figure 4, a thick dashed line delineates the region where Δ>0.1. The region left from this curve corresponds

to a significant slowing down of the initial drop velocity by the work of the drag forces, while the region right from the curve correspond to a negligible effect of the drag forces on the initial drop velocity.

Note that the terminal velocity of a droplet is the velocity at which drag forces and gravity forces are in balance (the violet curve in Figure 4).

b4. Will the drop accelerate or slow down?

This question is best solved by comparing the respective magnitude of the drag force and the gravity force. This ratio is expressed with the dimensionless number

$$\Gamma = mg/F_D \,. \tag{7}$$

In the above equation, the drag force can be analytically calculated based on the initial velocity from eq. (2). In Figure 4, the black dash dotted line delineates the region where $\Gamma < 1$; above that line drag forces dominate and the drop slows down; below, gravity dominates and the drop accelerates. The terminal velocity of a droplet corresponds to the situation where gravity and drag forces are in exact balance. It is a function of the droplet diameter and is indicated by the violet curve in Figure 4.

As a summary, the following physical regimes correspond to specific regions (numbered from 1-6) in Figure 4.

Physical Regime	Physical Significance on the Trajectory of a Drop
1	Significant acceleration of droplet due to gravity forces, drag forces are significant
2	Significant acceleration of droplet due to gravity, drag forces are insignificant
3	Minor deceleration of droplet due to drag, gravity negligible with respect to drag, but gravity significant with respect to initial kinetic energy
4	Drag forces significantly decelerate the drop; gravity negligible with respect to drag, but gravity significant with respect to initial kinetic energy
5	High probability that drop breaks up into smaller drops during flight, due to shear breakup
6	major deceleration due to drag; gravity negligible with respect to initial kinetic energy

Table 3: Significance of the physical regimes, shown as specific regions in Figure 4

While Figure 4 has been drafted for the pedagogical purpose of showing the use of dimensionless numbers, similar regime maps are important tools to discriminate situations where gravity and drag forces matter, from situations where these do not matter. This might be relevant to the selection of methods to reconstruct the trajectories of blood drops.

(c) Dimensionless numbers are useful for designing experiments. For instance a large blood drop impacting a target at low velocity might behave in exactly the same way as a smaller drop impacting a target at higher velocity. *While the latter experiment might be very hard to make, the former might be easier to make.* The fundamental reason behind this is that two physical events will behave in a similar way if the ratios of physical forces are the same, i.e. if the values of the relevant dimensionless numbers (here, the Reynolds number as well as the other relevant numbers) are matched, see point (b) above. For more details on the use of dimensionless numbers, see the discussion on similarity and dimensional analysis by Sedov and Taylor [38, 39].

As a summary, the use of dimensionless numbers helps to
(a) replace multiple dimensional plots by a single dimensionless plot;
(b) determine what physical forces influence a specific phenomenon (here the impact velocity of a drop), and what physical forces can be neglected; and
(c) design experiments

3. Drop generation

3.1. Description in the BPA literature

BPA experts often describe single stains or *spatters* (group of stains) with a terminology that indicates the most probable mechanism of their generation [5]. These terms, with several other commonly used in BPA, are defined in Table 4. The terminology is based mainly on the recognition of typical spatters, in terms of their spatial distribution, the size distribution and orientation of their stains (for example converging radially or aligned). Indeed, a beating causes several individual and clearly visible mm-stains, while a shooting causes a preponderance of sub-mm overlapping stains, a pink layering called "pinking" or atomized mist. For example, the terms *drip stain* refer to drops that fall when their weight overcome capillary forces, while *cast-off patterns* refer to spatters of drops generated when acceleration forces overcome capillary forces. Other spatter terminology hinting at the generation mechanism include *impact pattern, mist pattern, back spatter pattern, forward spatter pattern, pool, swipe pattern, splash pattern, bubble ring, projected pattern* and *expiration pattern*. These spatters of known origin are routinely generated and studied in the workshops educating the BPA examiners.

Two assumptions have been used in BPA studies to correlate the size distribution of stains in the spatter to the mechanism that generated the spatter:
1) the stain size correlates inversely with the momentum or speed of the generation event [4];
2) the stain size indicates the drop size (see discussion in section 5.1.2). For instance, [43] mentions that "The mass of the blood drop can be estimated approximately by the diameter (width of the bloodstain) and the density of blood."

The direct observation of the dynamic generation of a blood spatter is challenging, because of the high speeds involved (a baseball bat swings at more than 30 meter/second [44]) and the sizes of the objects to monitor (sub-mm drops are produced in a gunshot spatter). Early attempts of high-speed visualizations in BPA have been reported in 1939 [42], when the oblique impact of mm-size drops was recorded with an analog camera at speeds up to 250 images/second. The report [42] mentions two difficulties: the need for lot of lighting, and the difficult synchronization between the recording and the event. The more recent video "Blood in Slow Motion" [45] shows

recording at 4000 images per second. The sequences show the formation of blood drops, normal and oblique impacts on solid surfaces of various roughnesses and porosities, impacts on liquid blood pools, and the formation of castoff spatters. With the advent of digital high-speed cameras in the late 1990's, the issue of synchronization has been mitigated, and speeds up to 1 million frames per second have been made possible. For instance, strobe photography and high-speed camera visualization have been used in BPA for expirated [46] and gunshot spatters [47, 48]. In the latter case, information was gathered on the complex interaction between the air flow induced by the gunshot and the flight of the cloud of sub-mm droplets. The best examples of digital high-speed videos related to BPA are the extensive studies [48, 49] done by Epstein, Laber and Taylor. The related publicly available dataset [50], which is the source of Figure 6 and Figure 10, has brought attention in the BPA community to the complexity of the associated fluid dynamics phenomena.

3.2. Fluid dynamics description

Fluid dynamicists have a long tradition in studying the generation and impact of drops for the purpose of technologies such as fuel atomization, ink-jet printing, additive manufacturing, painting, agriculture, or for the intellectual pleasure of understanding how nature works. These studies involve sketches by *da Vinci* [51], Savart [52] and Worthington [53], see Figure 5 A-B. Drawings by Worthington are the first examples of high-speed visualization of drop impact, and a remarkable testimony of mankind's creativity. In the late 1800s, Worthington used short and intense electric sparks to impress his retina and 'freeze' the motion of impacting water and mercury drops. Patching together several of these sketches taken at different instants of the impact, he could sketch without camera a sequence of drawings of drops deforming during impact, achieving a time resolution better than a millisecond [53, 54]. Current commercially available high-speed cameras can conveniently record continuous movies from events at frame rates up to 100,000 frames per second [55]. Using similar principles as Worthington, but faster flashes and sensitive cameras, FD phenomena have been imaged in research laboratories at frame rates up to one million frames per second [56]. Femtosecond lasers provide even faster illumination, and frame rates up to one *trillion* frames per second are even possible [57], as long as the investigated phenomena are reproducible at these timescales.

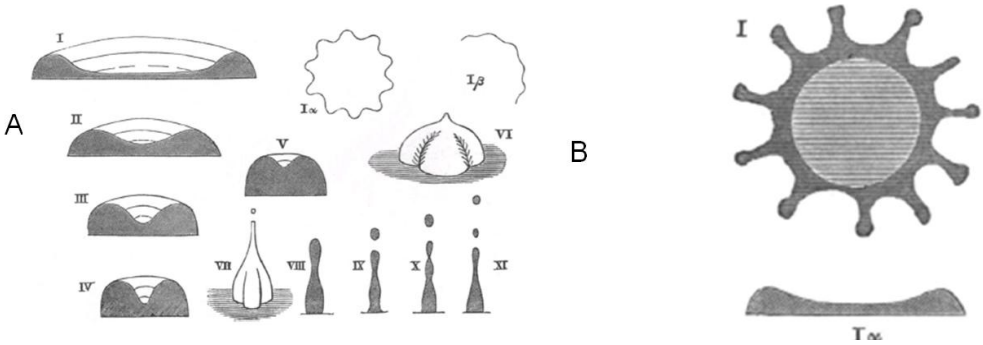

Figure 5: Early attempts of visualizing drop impact. (A-B) show various shapes assumed by a drop of milk impacting on a glass target, as sketched in 1876 by Worthington, without a camera, but with the help of an electrical spark generator and of his retinal persistence. Hand-drawn sketches show ring accumulation during the impact, splashing and the formation of spines [53, 54].

Several other non-intrusive experimental technologies are applicable to measure the dynamics of drop generation, flight and impact, in terms of particle size, velocities, temperatures, composition and their distributions, as reviewed in [58-60]. The technologies include particle image velocimetry, laser-induced fluorescence and laser-Doppler methods.

The dynamics of drop generation is also well documented for the following processes: dripping, sheet breakup and jet breakup.

Dripping occurs when a slowly growing volume of liquid suspended by capillary forces is detached as a drop by gravity forces. Inertial forces typically play a secondary role because the process is slow. The debate [40, 41] in the BPA community about the existence of a typical or minimum volume of a blood drop generated by dripping can be resolved as follows: this volume depends on the balance between gravity and the vertical projection of the capillary forces, rather than simply on the balance between gravity and surface tension. While surface tension only depends on the solid and the fluids in contact, the vertical projection of the capillary forces depends also on the wetted diameter and wetting angle (see Table 2), i.e. on the shape and material of the object from which the drop drips. Therefore, dripping drops with a wide range of volumes can be generated by changing, for example, the diameter or material of a pipette, as already mentioned in the French version of the early BPA work of Balthazard et al. [42].

The dripping phenomenon is well understood [61, 62], in terms of kinematics [63], frequency, drop volume and "pinch-off length", which is the distance where a drop separates itself from its source. Viscosity influences the dripping process of Newtonian [64] and non-Newtonian fluids [65]. If the flow rate that causes the initial volume of liquid becomes faster, inertial forces come into play (as indicated by non-negligible Weber numbers). Inertial effects affect the drop size, the formation of smaller "satellite" drops [66]. At even faster flow rates dripping transitions towards jetting, when the Weber number reaches a critical value [67]. Also, dripping and jet breakup induce longitudinal oscillations in the generated drops [68, 69]. The frequency of these oscillations is controlled by surface tension and the mass of the drop [70], and viscous forces tend to dissipate these oscillations.

Sheet breakup: In several situations relevant to BPA, the blood spatter originates from a liquid sheet that subsequently experiences several topological changes until it breaks into drops. Complex instability mechanisms drive these topology changes, from sheet to jets, and from jets to drops as shown in Figure 6. These topology changes are important, because they indicate that there is no such thing as a single "point" of origin of a blood spatter. Sheet breakup has been studied in relation to commercial nozzle and spray generation processes, as reviewed by Lefebvre [71], and also in relation to its occurrence during drop impact (see section 5.2). The generation and breakup of liquid sheets are visible during drop generation processes such as the coughing of blood shown in Figure 6, or during the impact of a drop on a wet surface [72]. The breakup of a sheet involves a cascade of events, such as (1) the thickening of the forward edge of the sheet into a cylindrical rim, due to the tendency of interfaces to assume a spatially-uniform curvature, forming either plain cylinders or spherical drops; (2) transverse instabilities on the rim, leading to cusps and finger-like jets; and (3) longitudinal instabilities along the rim, such as the Plateau-Rayleigh [24] instability that break the jets into drops, as in Figure 6d.

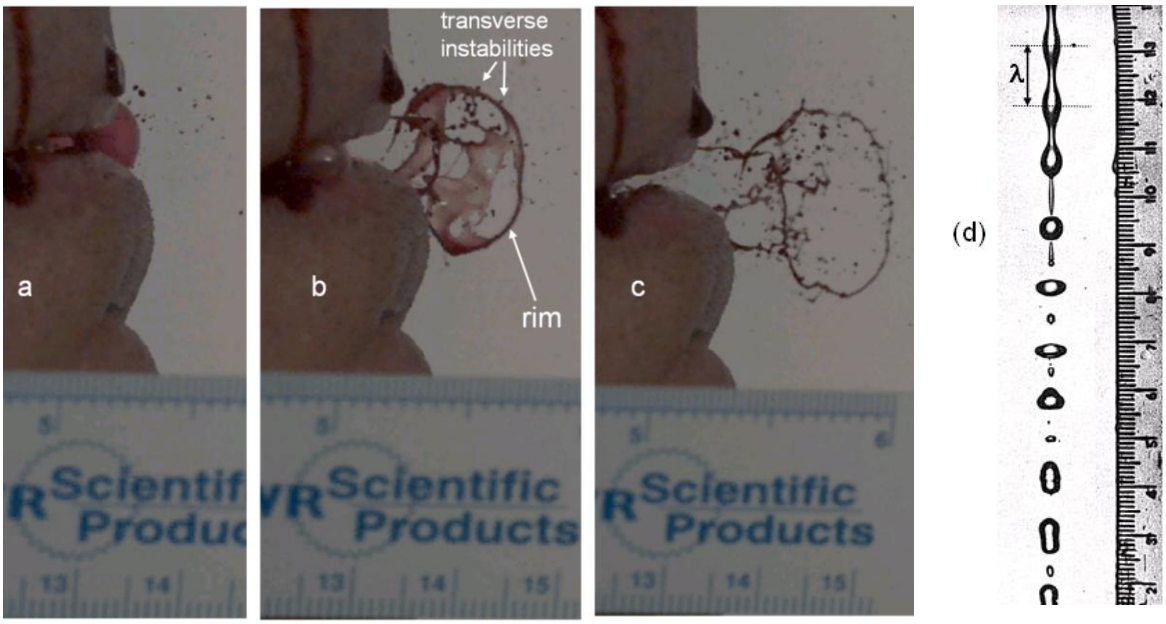

Figure 6: (a-c) High-speed visualization of the cascade of events leading to the formation of drops during the breakup of a liquid sheet, reproduced with permission from the Midwest Forensic Center [49, 73]. Plateau-Rayleigh instabilities tend to minimize surface area and can break a liquid jet into drops, as in picture (d) reproduced with permission [74, 75].

Sheet breakup is more complex than dripping. The time for the sheet to breakup can be estimated using linear stability theory [76, 77]. Also, experiments and fluid dynamic models on atomization [78-80] relate the average size of drops to a power of a characteristic Weber number $We=\rho V^2 L/\sigma$, where L is a representative length scale of the initial configuration, for example the thickness of the liquid sheet.

Jet breakup: The formation of drops from a liquid jet occurs by several instability mechanisms that break the jet into a train of drops, as e.g. in Figure 6d. These mechanisms are reviewed in [23, 81]. Instabilities are characterized by their driving and resisting forces, their temporal evolution (growth rate) and their spatial features (wavelength λ). Understanding how instabilities grow helps to determine the time of breakup and the size distribution of the drops.

4. Flight of drops

4.1. Description in the BPA literature

One of the main issues in BPA is to determine *where* a blood spatter originates from, for the purpose of reconstructing the bloodletting event. This operation involves the backward reconstruction of drop trajectories based on the inspection of the stains, and on a model for the flight of drops.

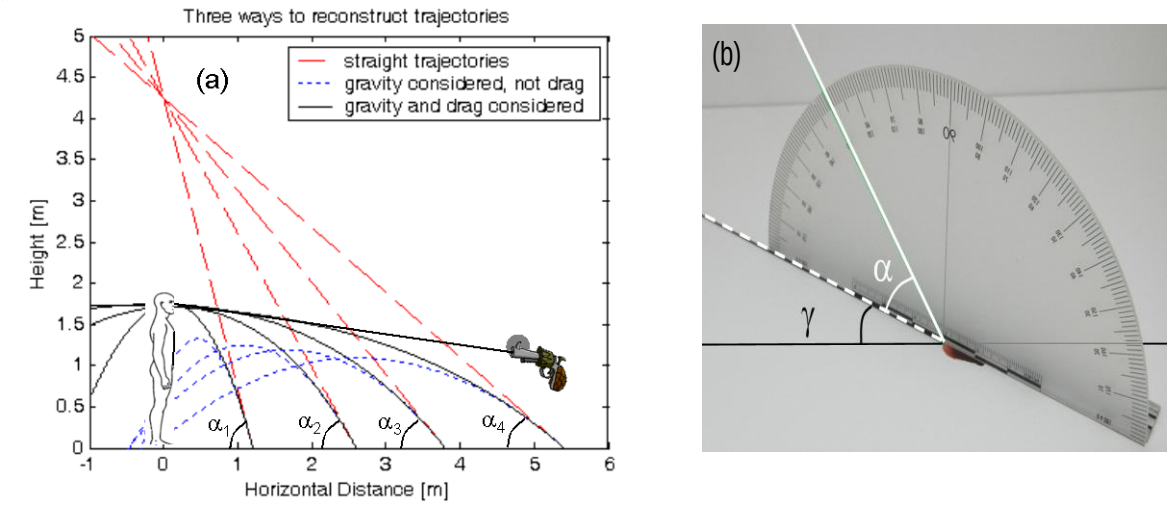

Figure 7: (a) Reconstruction of the trajectories of four bloodstains using straight trajectories vs. ballistic trajectories; the geometry (locations of the stains, of the victim, impact angles) in (a) is reproduced from teaching material graciously provided by H. McDonell. Drops size is assumed to be 3mm, implying velocities in the interval 5.3-7.5 m/s. (b) definition of the angle of impact α and directional angle γ.

The terminology used for trajectory reconstruction is illustrated in Figure 7 and defined in Table 4. The three-dimensional region of origin of a blood spatter is called the *area of origin*, and its normal projection onto a horizontal plane is the *area of convergence*. The area of convergence corresponds to the intersection of straight lines with direction γ, linear projections onto a horizontal plane of the ballistic trajectories of the blood drops. To determine the area of origin, BPA experts use the *angle of impact* α from several stains using the visual inspection methods of section 5.1. This angle is the acute angle at which a blood drop strikes the target, see Figure 7b. As an example, in Figure 7a, the area of origin, target plane and area of convergence are respectively the region near the head of the victim, the floor and the area on the floor supporting the feet of the victim; labeled as $\alpha_{1\text{-}4}$ are the four angles of impacts.

An early BPA study on the relation between impact spatters and the area of origin is the graphical work of Piotrowski (1895), extensively reproduced and commented in [82]. The work describes among others the spatial distribution of stains created by a hammer impacting a pool of blood, and the blade of a hatchet hitting either a rabbit head or blood-soaked cotton cloths. Piotrowski observed that the orientation of the stains can indicate the origin of the blood spatter. Both Piotrowski's and Balthazard et al.'s [42, 82] work specify that bloodstain trajectories are not straight lines, a concept also reflected in the BPA literature by mention of 'bent trajectories', 'ballistic trajectories' or 'parabolic trajectories', to acknowledge the influence of gravity and drag forces.

As stated in 1939 in Balthazard et al., [42] "*Le problème* [of reconstructing trajectories] *est très difficile à résoudre*". Indeed, reconstructing trajectories is still very difficult today. A first-order approach to reconstruct trajectories is to assume that the droplets travel in a straight line. Reconstruction methods based on straight trajectories, such as the method of strings or the trigonometric method, have been used in crime scene reconstruction since at least the 1950s [83] and have been implemented in software routinely used in crime scenes [84-88]. There is abundant BPA literature on the uncertainties associated with the choice of stains and their inspection to determine the angle of impact and area of origin [89-93]. The uncertainties are of two types, the error induced by assuming linear trajectories, and the uncertainty in determining the angles γ and α from stain inspection. Uncertainty on α has been reported to stem from the asymmetrical nature of bloodstains, the inappropriate use of a protractor [94], or the measurement of the length and width of the stains [95, 96]. Also, [97] reports errors on the determination of the region of origin larger than 44 cm due to the assumption of straight trajectories. Similarly [15] verifies experimentally that the stringing method "over-estimates the point of origin and the error associated with this technique is significant (50% on average)." Such error is significant enough to wrongly conclude that a person was standing when in fact they may have been sitting. BPA experts are well aware that the area of origin is determined in an approximate sense [4], either as a maximum height from where the drops could originate, or "*within the volume of a grapefruit, or even a basketball*". This level of accuracy is considered satisfactory for many crime scene reconstruction purposes [4].

Recently, BPA research has proposed methods to reconstruct curved trajectories. Buck et al. [43] reconstructed drop trajectories using ballistic calculations, considering gravity and drag forces. In their ballistic analysis, they screen a range of velocity values for compatibility with the preservation of the drop during the flight (no breakup by drag overcoming surface forces, see Figure 4). Some assumptions associated with their analysis are discussed in [98]. [99] describes "a method of reconstructing the area of origin in a nonlinear manner", that incorporates the effects of drag into trajectory calculations, using probability densities. Finally, a statistical procedure [100] based on aggregate statistics and the basic equation of projectile motion has been shown to determine the area of origin of a blood spatter for cases when the spatter is launched within a narrow range of polar angles. Since ballistic reconstruction involves the knowledge of impact velocity and drop size, a significant amount of recent BPA work has focused on obtaining that information by inspecting the stains, as discussed in section 5.1.

A crime scene can be confusing, and stain selection is important in determining the area of origin. Typically, the crime scene investigator selects stains based on the following criteria: accessibility, adhesion to the target surface, abundance, and relative location [97]. Once these stains are chosen, their location is measured, the stains are photographed as a basis to determine their directional and impact angles, so that the areas of convergence and origin of the blood spatter can be determined.

BPA researchers are also aware of two bounds on the velocities of drops: (1) drops will break if drag forces overcome surface tension forces [43], and (2) gravity will not accelerate a drop in still air beyond the terminal velocity [101], which is provided in Figure 4.

Recent BPA work has identified two limitations of the ballistic reconstruction of trajectories:
1) The area of origin of the drops is distinct from the area of origin of a blood spatter, because the drop generation process involves a sequence of topological changes, such as, for example, during the breakup of a liquid sheet [13].
2) The air through which the drops fly is not always at rest; sometimes the air plays an active role in the transport of drops. In that case, equation (1) is still valid to calculate the trajectory, but the velocity used in the related equation (2) is the velocity difference between the drop and the

air. For instance, experiments involving respiration-caused blood spatters have demonstrated the importance of understanding the role of the surrounding air [102], which helped carrying sub-mm drops further away than occurs in still air.

4.2. Fluid dynamics description

The trajectory of drops has been studied in several applications of a subfield of FD called multiphase flow [58, 103-106], relevant for example to spray painting, inkjet printing, fuel sprays, meteorology, medical sprays, and the fabrication of micro-particles. Typical topics of interests in multiphase flow are the generation and control of desired distributions of drops size and velocities. The relevant physical parameters and forces are the same as in BPA, the surface tension and viscosity, the drag and gravity forces, and their effects on the drop velocity, shape and temperature. As reviewed in section 3.2, a wide array of experimental tools [58-60] are used by the multiphase flow community to characterize the trajectory of drops and of clouds of drops.

Figure 8 builds on the model problem of Figure 7, which relates to the reconstruction of ballistic trajectories. For the sake of simplicity, the air is assumed quiescent. In that framework, the trajectories are governed by equations (1) and (2). To solve these equations and reconstruct ballistic trajectories, values of the impact angles, impact velocity and drop size are needed.

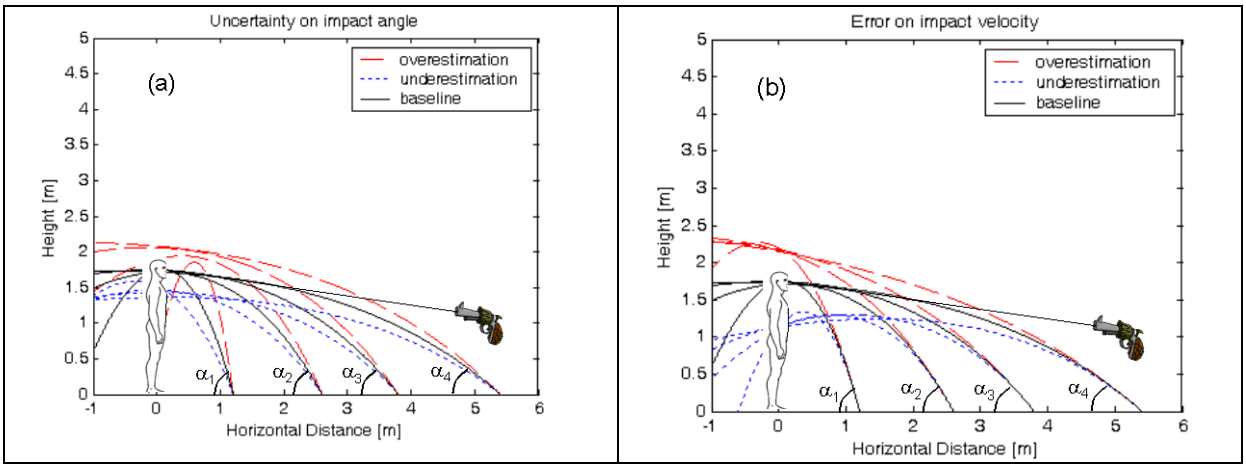

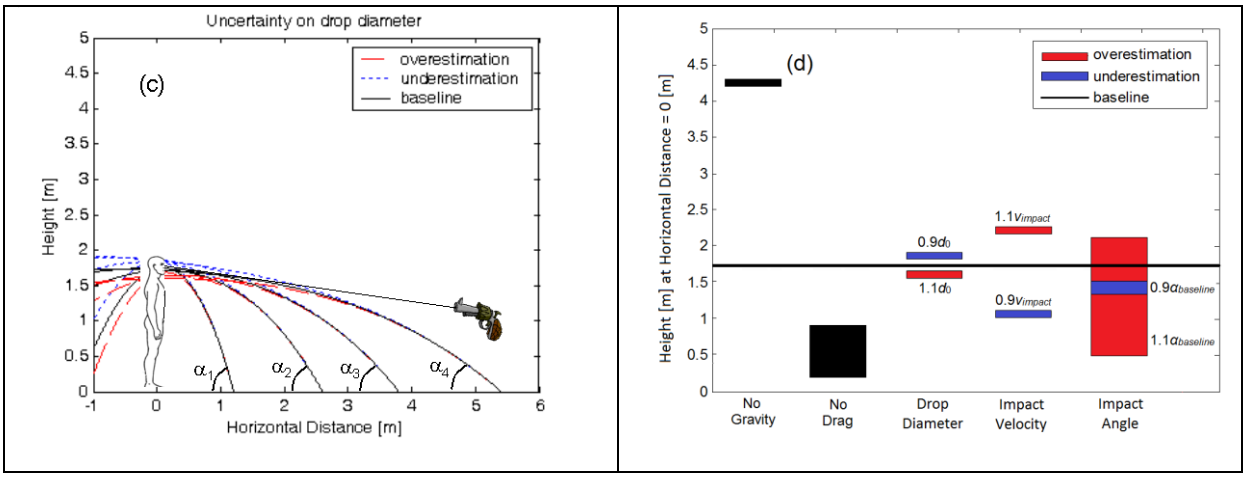

Figure 8: Examples of how uncertainties on physical parameters influence the determination of the area of origin of a blood spatter: (a) Effect of uncertainty in the impact angle; (b) effect of uncertainty in impact velocity; (c) effect of uncertainty in drop diameter; d) estimated heights of area of origin for initial conditions reported in Figure 7 and Figure 8. In figures (a-c), the baseline case is the same as in Figure 7, while a representative error of +10% is assumed for the *overestimation* curve, and of -10% for the *underestimation* curve.

Parametric studies in Figure 8 illustrate how uncertainties on the impact angle, impact velocity and drop diameter influence the determination of the region of origin of that specific blood spatter. To do so, the baseline case (black curves) is modified with a typical uncertainty on the impact angles (top right), on the impact velocity (top right) and the drop size (bottom left). The value of the typical uncertainty is set to +/-10%, as it is representative of uncertainties in the measured the impact angle [95, 96], the droplet impact velocity [107] and diameter [107], the latter two being determined with the method of spines. For the specific BPA example in Figure 7 and Figure 8 the largest errors on the determination of the area of origin are shown in Figure 8d, and come from (in order of the magnitude of the effect): neglecting gravity (error of several meter), neglecting drag, uncertainty on the impact velocity and impact angle, and uncertainty on the diameter of the drop.

Calculations of trajectories are not trivial because flying drops do not behave as rigid particles: they might deform or break up in smaller drops when the drag forces become comparable with the surface tension forces, as explained in section 2.2.1(b1). Recombination and oscillations might occur during flight, see section 3.2, affecting the drag, the calculation of trajectories as well as the stain shapes and sizes [19, 108, 109]. Another concept important for the reconstruction of trajectories is the notion of terminal velocity, described in section 2.2.1(b3). Also, when droplets are generated at velocities comparable to the speed of sound, e.g. by

gunshot, the drag coefficient depends on the compressibility of the air. In that case, correlations used in rocket design could be used [110] for the estimate of the drag force.

It is also important to mention that blood spatters originate from blood at body temperature (37°C) that typically travels through colder air and impacts a colder target. To the best of our knowledge, the issue of the cooling of the droplet in flight and during impact [111] has never been addressed in the context of BPA, as shown in Table 4. This issue might be important because the physical properties of blood vary considerably: when cooled down from 37°C to 20°C (Table 1), the viscosity and surface tension increase by 60% and 27%, respectively. Such large changes of physical properties affect the Reynolds and Weber number, which might affect in-flight atomization, drop spreading, spine formation and splashing.

A related issue is the evaporation of drops during flight, which might be most important for small drops travelling at large velocities, because of their higher surface to volume ratios.

5. Impact

5.1. Description in the BPA literature

As early as 1939, Balthazard et al. [42] pioneered the scientific investigation of drop impact for BPA, investigating experimentally and rigorously how the fall height of a drop influences the shapes of stains, for both normal and oblique impact. These authors took care to discriminate interesting findings from useable findings, and the recorded the first high-speed movies of blood drop impact. Indeed the relation between the shape of a stain and the impact conditions of the related drop is key for reconstructing trajectories.

As of today, impact is probably the best understood of the four chronological stages described in this review (drop formation, flight, impact and staining). An excellent exposition of the current knowledge in BPA on drop impact of drops is available in the recent review of Adam [14].

Before the early 2000s, the BPA community named the blood spatters in relation to the speed associated with the spatter generation, with the terms of Low, Medium or High Velocity Impact Spatter [5]. The reason was to acknowledge an inverse correlation between the size of a distribution of stains and the magnitude of the velocity or momentum applied to the static blood to produce the spatter.

Later, this classification scheme was reconsidered after observing overlapping stain sizes between the Medium and High Velocity categories. A novel taxonomy, with examples in the left column of Table 4, was proposed by The Scientific Working Group for Bloodstain Pattern Analysis (SWGSTAIN, an FBI-founded international group). The taxonomy classifies the stains in three categories [5] based on the mechanisms driving the staining process: *passive stains* are caused by gravity as the only driving force; *spatter stains* are formed by additional forces besides gravity, such as the momentum of an impact, and *altered stains* exhibit the influence of physical or physiological events occurring *after* the staining process, such as cleanup attempts, decomposition or even flaking.

5.1.1. Normal impact

When impact angle $\alpha=90^o$ (see Figure 7b), the impact is normal to the target. An impact under any other angle is called oblique, and will be treated subsequently as it involves a more complex and asymmetrical deformation of the drop.

Upon normal impact, the contact diameter between the drop and the target surface expands until it reaches as maximum, in a process called *spreading*. In [42], a relation was found experimentally between the height of a drop in free fall, and the diameter of the stain: the higher the fall, the larger the spreading and stain size. The simplest parameter to characterize the spreading is the *spread factor* $d_{max}/d_{0,}$ i.e. the ratio of the *maximum contact diameter* over the *initial drop diameter*. The spread factor has been estimated using first-order FD models [13, 112-114]. These models compare the various energy terms available before impact (kinetic, potential, surface) with energy terms available after impact, considering that some of the impact energy has been dissipated by e.g. viscous forces. Since spreading is typically driven by inertia and gravity and resisted by surface tension and viscous forces, the spread factor can be estimated with a relation of the kind, $d_{max}/d_0=f(Re, We, Fr)$, with the dimensionless numbers defined as in Table 2. Arguing that in several cases relevant to BPA, $We>>Re$ and neglecting the effect of gravity during the impact, Chandra's group proposed the correlation [114]

$$\frac{d_{\max}}{d_0} \cong \frac{1}{2}\mathrm{Re}^{1/4} \quad . \tag{8}$$

Relations developed with a similar approach are also in [11, 115].

By itself, the description of equation (8) is of limited use in BPA because the initial diameter of a drop is rarely known; however, the combined measurement of spreading and spines (below) can help estimate the impact conditions.

When the impact energy is large enough, that the edge of round stains are no longer smooth, but rather disturbed by *spines* – also called fingers, scallops, sunburst effect [116] or spikes – as shown in Figure 9a. Spines appear in increasing number as the impact velocity increases [42]. The instability mechanism responsible for the formation of these spines has only been investigated recently. Marmanis and Thoroddsen [117] developed a correlation between the impact Reynolds number and the number of fingers, *N*, and attributed the fingering to

interactions between inertial and viscous forces, see also [118]. Recently, Hulse-Smith et al. [114] proposed a correlation dependent on a target material-specific empirical coefficient, $C \sim O(1)$, and on the Weber number, i.e. the ratio of inertial forces (that enhance fingering) to the surface forces (that reduce fingering), where

$$N = C\sqrt{We}\,. \tag{9}$$

Reference [114] proposes to combine equations (8) and (9) to determine d_0 and v_0 based on the measurement of the stain size d_{max} and of the number of spines N, assuming that the material properties of the blood (ρ, μ, and σ) and of the target material (C) are known. That approach to determine the impact conditions from the inspection of a stain is known as the *method of spines*. A derived approach, independent of the physical properties of the blood, is described in [107] for impacts on paper, drywall and wood. Spines can merge or be indistinguishable from oscillations on the edge of the stain due to local changes of substrate roughness or wettability. As a result, there is an inherent subjectivity in determining the number of spines, leading to recommendation in Hulse-Smith and Illes [107] that only one individual count all the spines related to a specific BPA study. In [14], Adam also mentions two limits of applicability of the *method of spines*: the absence of spines for low-energy impacts and the saturation of the number of spines at high Weber numbers, see Figure 9b.

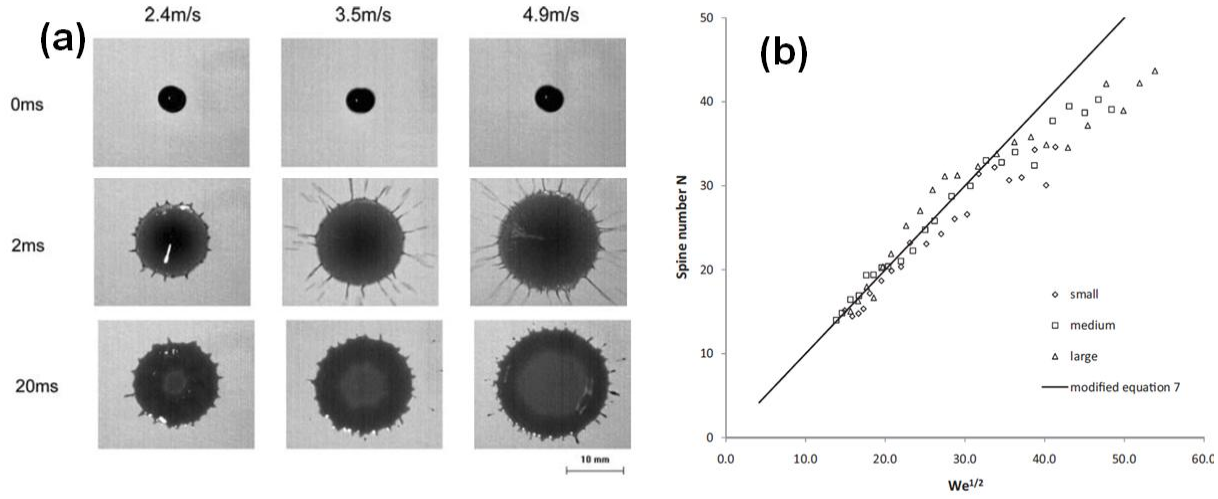

Figure 9: **Fluid Dynamics instabilities tell about the impact conditions. The number of spines radiating from the edge of a stain increases with the impact velocity (a), from [107]. In (b), [14] shows the dependency of the number of spines on the Weber number.**

The occurrence of *splashing* –the breakup of the drop into distinct amounts of liquid upon impact- can be explained in relation to the formation of spines. Since the formation of the spines is driven by inertia and resisted by capillary and viscous forces, three regimes can be identified in a Re-We plane (or in a v_0-d_0) plane. When the ratio of inertia over capillary and viscous forces is low, the drop spreads without scallops or spines. When that ratio becomes larger, the edge of the stain exhibits spines. When that ratio becomes critically large, instabilities grow to the point of breakup and splashing [118]. Quantitative criteria to discriminate between these three regions are described in [14].

Regarding the influence of the *target*, as documented by Balthazard et al. [42], its shape, material, preparation, structure and oxidation influence the spreading of drops, the formation of spines and of stains. Since most blood drop impact studies have been made on paper, the corresponding published BPA literature is only valid for impacts on paper targets. For instance, Balthazard et al. mention [42] that their results are only valid for impact on a specific type of cardboard paper. In [4, 119], MacDonell writes about how the substrate roughness can increase spatter, i.e. promote splashing. Studies [89, 114] compare blood drop impact on different substrates (glass, paper, steel and wood), with different roughness. Note also that a specific class of target surfaces is of specific importance for BPA: the clothes of either the perpetrator or the victim [120].

A large set of *high-speed visualization experiments* of normal and oblique impacts on various substrates, at various speeds, is available, with the techniques and from the sources mentioned in section 3.1.

Two *questionable assumptions* sometimes appear in BPA reports on the impact of drops:
1*) the stain area corresponds to the maximum contact area between the drop and the target during impact (=maximum spreading).* This is probably realistic for substrates that are hydrophilic, but not for hydrophobic substrates, such as greasy tiles, where the stain diameter can be smaller than the maximum diameter reached during impact, as clearly shown in [42]

2) *the stain diameter indicates the distance of fall [121], i.e. the impact velocity*: this is only true if the initial size of the drop is known, as was also clearly shown in [42].

5.1.2. Oblique impact

The oblique impact of drops on a surface is illustrated in Figure 10, and result in elliptical stains. The lateral spreading *W* (the minor axis of the elliptic stain, perpendicularly to the projection of the velocity vector on the target) is driven not by the whole velocity, but by the velocity component normal to the surface [14]. An equation similar to equation (8) therefore applies, where *Re* is defined based on the velocity component normal to the surface. The axial spreading, *L*, along the projection of the impact velocity onto the target plane is typically larger than *W:* while the velocity component normal to the surface induces axial spreading similarly as the longitudinal spreading, the cylindrical path of the droplet intercepts the surface at an angle α, and this latter contribution makes *L* larger than *W, so that the stain is elliptical*.

Experiments show that the ratio *W/L* of the extension in the lateral direction over that in the forward direction increases monotonically with an increasing impact angle [42], following a trigonometric relation established in [122]

$$W/L = \sin\alpha \, . \qquad (10)$$

Measuring the ellipticity of a stain therefore provides important information on the impact angle. The error using the formula (10) is estimated in [89, 121]. Note that elliptic stains do not necessarily imply an oblique impact, as any relative motion of the target perpendicular to the drop trajectory can cause a non-circularity in the observed stain, a fact studied experimentally in [123].

Balthazard et al. described that the impact velocity modifies the shape and number of *spines* at the forward end of a stain resulting from an oblique impact [42]. Knock and Davidson [124] propose an approach to determines d_0 and v_0 by inspection of the bloodstain size and the number of spines for oblique impact.

In relation to *splashing*, Pizzola et al. [41] describe the formation of a *wave-castoff*, this single satellite drop detaching from the forward end of the parent drop during an oblique impact.

Several recent publications on the impact of blood drops have related the outcomes (spine formation, stain diameter and shape) to impact conditions within a dimensionless framework [11, 14, 114]. For example, Adam [14] proposed that the observed impact behavior of blood droplets (i.e. gentle spreading into a smooth ellipse, appearance of scallops or spines, splashing into several drops) is controlled by the ratio of the inertia of the flow at the wetting line parallel to the target plane, over the stabilizing forces of viscous dissipation and surface tension. A similar theory was verified for Newtonian fluids [125] and explains why, in experiments where the inertia of the impact is gradually increased, scallops, spines and splashes are typically observed at the leading edge of a stain earlier than at the trailing edge.

A misconception concerning oblique impact is that *the stain width equals the drop diameter [90]*. This is not a universal truth as evidenced by $W >> d_0$ in Figure 10.

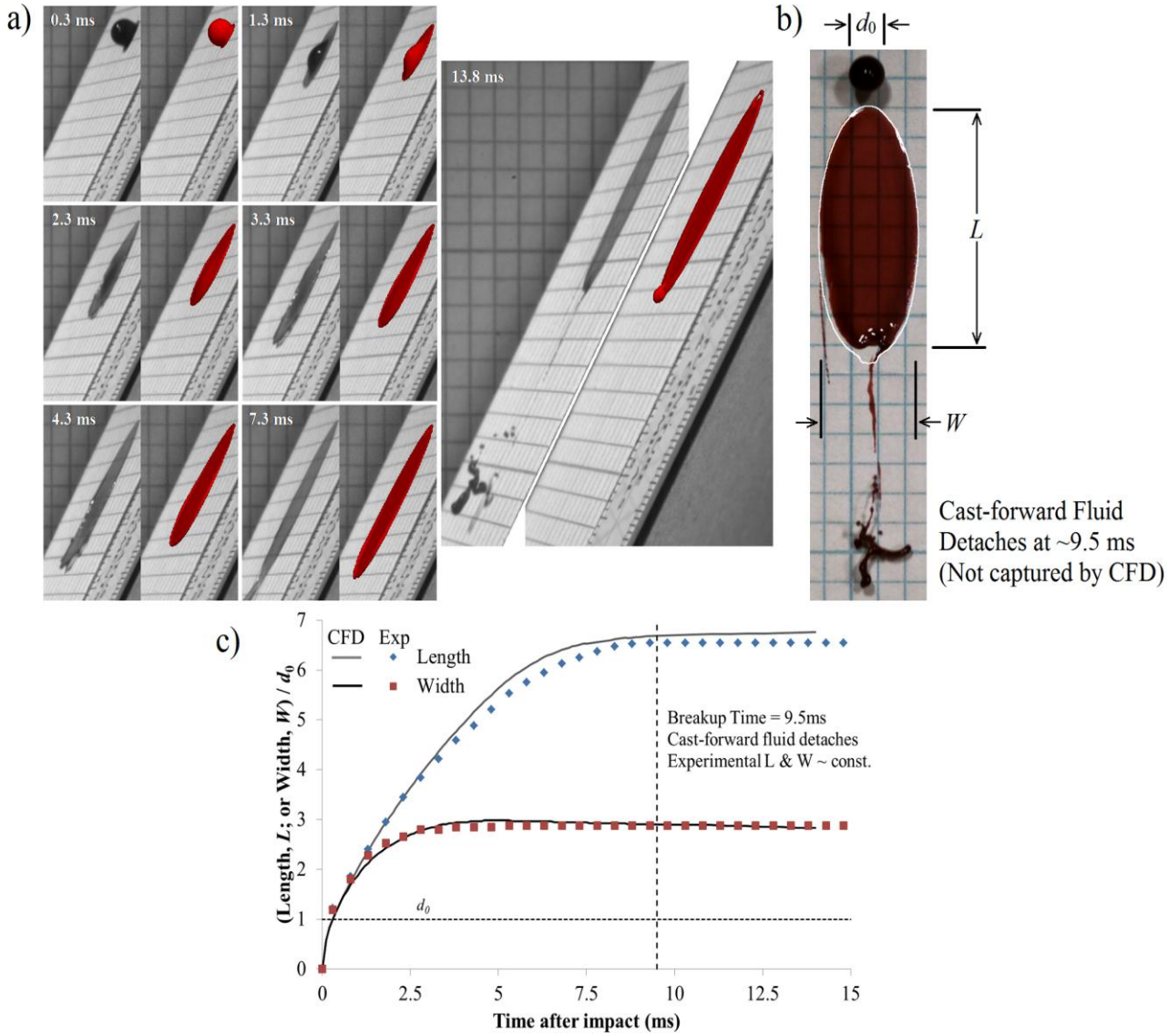

Figure 10 : Experimental and computer-based simulations of the impact of a 4 mm blood droplet striking an oblique surface at 28° and 4.3 m/s: Comparative droplet shapes (a) of experimental (left and grey) and simulated (right and red) for the indicated times after impact; (b) overlay of simulated (white outline) and experimental drop/stain shape prior-to impact and 13.8 ms after impact; and (c) variation with respect to time of *L* and *W* . The final experimental *W/L* elliptical ratio of 0.44 corresponds to α=26.1° from Eq. (10). Experiments adapted from the MFRC Bloodstain Pattern Analysis Video Collection, case 4Ac2 [50]; simulations from coauthors A.D. and D.A.

5.2. Fluid dynamics description

Several reviews of the fluid dynamics of drop impacts on liquid and solid surface are available in [126-128]. Upon impact, the fate of a droplet can have various outcomes, such as spreading,

splashing, bouncing, or a combination of these. These outcomes are reviewed here considering mostly normal impacts. As mentioned in section 5.1, the description of impact is quite extensive in the BPA literature, so the present section does not repeat what was exposed in details in section 5.1.

While FD researchers can use the same wide collection of experimental tools to describe drop impact as for drop breakup, there is also a mature FD discipline called *Computational Fluid Dynamics* (CFD), which can be presented as follows. CFD has been widely applied to drop impacts and offers research and teaching opportunities for BPA, as exemplified in Figure 10. The fundamental equation describing FD phenomena such as the impact of a drop of Newtonian fluid is the Navier-Stokes equation, the expression of Newton's second law, eq. (1). Because of its explicit modeling of the viscous dissipation inherent to fluid flows, the Navier-Stokes equation is a non-linear, second-order partial differential equation, quite difficult to solve with pen and paper. CFD methods are computer-based techniques to solve equations such as the Navier-Stokes equations. To do so, the volume (the deforming drop) and the time (for example, from impact to drying) of interest are divided into a large amount of small volumes and small time increments. The Navier-Stokes equations are then discretized, i.e. expressed in an algebraic manner, for each of the small volumes and times, reducing the complex partial differential equations into large amounts of algebraic equations that can be numerically solved with computers.

CFD studies on droplet impact process have been reviewed in [127]. These numerical efforts were pioneered by Harlow and Shannon in the 1960s [129]. Subsequent work added the effect of viscosity [130], surface tension [131], wetting [113] and heat transfer during impact [132]. Later, researchers studied numerically the evaporation of drops on solid surfaces, see section 6.2.

There are currently no simulation tools that solve both the impact of a drop and the formation of a stain, but current simulation techniques are ready to address this challenge. These simulation tools could be used for investigating parameters that are difficult to investigate experimentally, such as the influence of viscosity, substrate wettability, or drop sizes and velocities that are relevant to crime scenes, but difficult to reproduce experimentally.

An example of current capabilities of Computational Fluid Dynamics is shown in Figure 10a. Input parameters of that simulation are the target wettability and the impact conditions. These preliminary three-dimensional simulations incorporate a dynamic wetting model [133, 134]. The simulation of oblique impact of a blood droplet on a paper target shows similar features as the experiments. For example, the simulated evolution of the wetting line, i.e. the motion of the boundary of the stain, closely matches the experimental data.

The spatial and temporal resolutions of the simulation in Figure 10 are however insufficient to capture the surface instabilities and the subsequent splashing observed at the leading edge of the impacting droplet, visible for times 3 to 10 ms. In that context, it is important to mention that simulations are not a panacea, because of the difficulty to model phenomena such as spine formation or wetting, which feature significantly smaller time scales or length scales than the typical scales used in the simulation. CFD simulations are indeed numerical representations of the continuum reality and necessarily partition the time and space with a given *resolution,* in a similar way as a digital picture partitions the real object with a given resolution of pixels.

To accurately estimate the *spreading* with equation (8), the viscosity of the blood needs to be known. In contrast to Newtonian fluids like water and liquid metals, the viscosity of blood is reduced by the high shear rates experienced during the impact process. In fact, during the early stages of the impact, for geometric reasons, the fluid velocities can be orders of magnitude larger than the impact velocity [127]; also, at large Reynolds numbers, the drop spreads into a very thin film surrounded by a donut-shaped ring where fluid accumulates [135]. The combination of large velocities and a thin film induces very large shear rates during the impact, causing the viscosity to decrease significantly. This begs the questions: *what viscosity value should be used to calculate the droplet Reynolds number for describing impact conditions?* This question can be answered as follows. The viscosities provided in Table 1 are for shear rates on the order of several hundred s^{-1}, above which the dependence on shear is somewhat limited, since thinning has already occurred. Considering that most viscous energy dissipation during impact would occur in a thin film jet (length scales below 1 mm), the shear rate would likely be at least on the order of 1 m/s / 0.001 m, or 1000 s^{-1}. It is thus reasonable to assume that the initial droplet

spreading characteristics can be described by the high-shear viscosities provided in Table 1. Note that the latter stages of droplet spreading and the staining process occur at much smaller velocities and shear rates, and therefore proceed at much higher viscosity.

In [126], Yarin describes the threshold condition which determines whether the drop spreads or *splashes* upon impact, based on considerations of the physical forces exposed in 5.1.1. Splashing typically occurs after a circular sheet or "corona" is formed [136]. The criterion to discriminate between spreading or splashing is

$$Re \cdot We^2 = K^4 \,. \tag{11}$$

where K is a target-dependent empirical constant, estimated as 57.7 in [136]. The influence of the substrate on the spreading and splashing has been studied in [126, 137-141]. Recent research by Nagel's and Brenner's groups has identified that the compressibility of the gas, here air surrounding the droplet [142, 143] affects the splashing. For typical BPA situations, their results agree with the criterion of equation (11).

In 1967, Ford and Furmidge [144] considered the influence of *target* wettability on the impact and spreading of drops. As discussed in section 2.2, the target elasticity –even the hardest glass or metal have some degree of elasticity- also influences the splashing. Lesser showed analytically [145] that during impact, the onset of sideways jetting of liquid from beneath the drop will be delayed by an elastic response of the wall, a phenomenon confirmed experimentally [146]. Rein [128] reviews that the elastic response of most surfaces has no influence at low velocities, but becomes important during high-speed impacts.

Importantly, the *wetting angle* (see Figure 2) is not a constant during impact as described in [133]. The wetting angle is also function of the direction of motion of the wetting line (advancing or receding), and of the relative speed between the wetting line and the substrate (or the capillary number). This dynamic behavior of the wetting angle influences the spreading and is still a topic of current FD research [133, 147-150].

Upon impact, the liquid contained in the drop might fully or partially *bounce* away from the wall [126, 151-153]. A correlation in [154] predicts the volume of Newtonian liquid that will be retained on a solid surface, based on the difference (or hysteresis) between receding and advancing wetting angles.

The impact of drops on liquid surfaces has been reviewed in [128], and involves the deformation by the impacting drop of the free surface of the liquid into a liquid sheet. That protruding liquid sheet, sometimes in the form of a crown, might break up into drops, by instability mechanisms described in section 3.2. Impact on liquid surfaces is important for basic FD studies on, for example, the noise of rain, and also for drip patterns in BPA.

6. Staining

This section focuses on how the stain forms, after the impact has deformed the drop. In other words, non-inertial aspects of the fluid transport are discussed, since inertial aspects (spread factor, impact angle, fingering, splashing) associated with the impact have already been discussed.

6.1. Description in the BPA literature

The *uneven thickness* of stains was described by Balthazard et al. [42], who noticed that the periphery of stains is typically thicker than their center. The authors guessed (rightly as shown in the late 1990's [155]) that the depressed center is rather due to some phenomenon occurring during the drying phase rather than to the presence of air bubbles in the impacting drop. The same work [42] commented on the presence of scale-like structures in the crust of the stain, and noticed that the appearance of the crust depends on the type of blood used, either real blood or blood with anticoagulant. They also mentioned that stains resulting from oblique impact are inhomogeneous, the bottom part being "crust-like" and dark, while the upper part is pink.

Balthazard et al. [42] studied how *capillary forces drive blood into fabrics*, noticing faster imbibition rates along the fibers than across. Kirk [120] also notes that some bloodstains go straight from the generation to the staining phase, describing the case of a stabbed woman whose blood had flowed between her breasts and into her clothing.

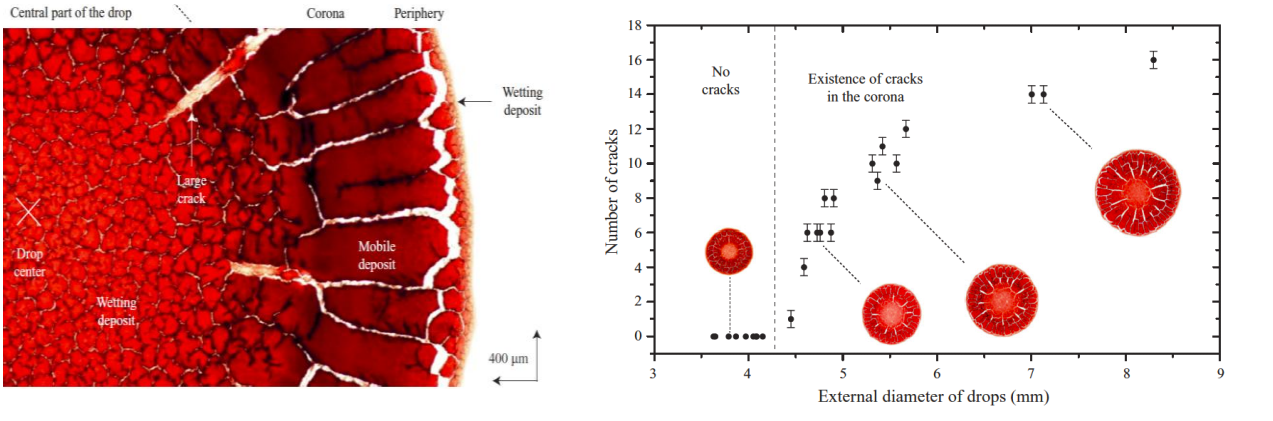

Figure 11: A magnified stain reveals a wealth of features; some of these features, such as cracks in the corona, are of interest to determine the impact or drying conditions. Images from [156], permission requested.

During drying, stains might suddenly detach from certain targets. This *alteration* process called delamination or warping is caused by radial stresses due to the shrinkage of the stain, which overcome adhesive forces between the blood and target. This effect occurs on smooth plastic sheets, but not on some rougher plastics as described in [42]. Another alteration process is described in the fascinating study [157] on how insects modify the shape of existing bloodstains or create artifact bloodstains.

Kirk [120] also describes methods to *identify* if a bloodstain comes from the perpetrator or from the victim (a question resolved later by genetic testing), as well as methods to spot bloodstains on backgrounds where stains do not stand out. Several chemical, physical or optical methods have recently been developed in BPA for detecting weakly visible stains, using functionalized nanoparticles [158] or Raman scattering [159], and for determining the age of bloodstains, as reviewed by Bremmer et al. [160].

6.2. Fluid dynamics description

Blood is not only a fluid containing particles (complex fluid), it is also a fluid initiating coagulation as soon as it flows out of the human body. Once the kinetic energy associated with the impact has dissipated, the formation of a stain on a solid, impermeable target, depends on the following physical processes: wettability [161], evaporation, viscous dissipation and coagulation. Reference [162] discusses the relationship between the rheology of the blood and the stages of blood clotting. Reference [12] describes the effects of various anticoagulants on the trail length left by a drop running along an inclined surface.

The formation of stains during the drying of complex fluids has recently become the focus of fluid dynamics studies motivated either by the ubiquity of this natural phenomenon, or by manufacturing applications called evaporative self-assembly. For instance, the formation of rings at the periphery of stains has been explained in [155] by the combination of a radial flow driven by enhanced evaporation at the wetting line, and pinning of the same wetting line by accumulation of particles carried by the radial flow. The evaporation of a drop of a complex fluid

such as blood is a typical multiphase process, featuring a *cascade of dimensional transport phenomena*: wetting at the *(1D)* wetting line drives the motion of the *(2D)* solid-air interface, where surface stresses due to chemical or thermal non-equilibrium such as Marangoni stresses [97] drive the bulk flow *(3D)* inside the drop. Several fluid dynamic studies have addressed either experimentally or theoretically the interplay of transport phenomena during drop drying and stain formation [163, 164]. For instance, Hu and Larson [165, 166] modeled the evaporation of a drop of pure liquid with a pinned wetting line. Simulations of the formation of stains have recently been performed [167-170]; this requires solving the motion of the liquid and of many suspended solid particles. This is a non-trivial task, because of, for example, the interaction of the particles with the wetting line [170].

The formation of stains on porous targets like fabrics and garments involves the additional complexity of *imbibition*. Imbibition is the transport of blood into the fabric, driven by wetting forces and resisted by viscous forces. For one-dimensional imbibition, for example the imbibition of a large cloth dipped normally into a pool of blood, the wetted length evolves as the square root of the time [171]. Some analytical results for more complex geometries are referenced in [172]. Reference [173] discuss the effect of surfactants on the ability of a liquid to spread into a fabric.

The formation of *cracks* on stains has been studied in [174]: Allain and Limat showed that the spacing between the cracks was controlled by the competition between the mechanical relaxation due to the opening of a crack, and the increased mechanical stress due to the enhanced evaporation across the walls of the crack. Brutin et al. ([156], Figure 11) propose a relation between the density of cracks in the crown and the initial drop volume.

7. Synthesis of the relationship between BPA and FD concepts, summary table and research opportunities

Section 2 describes the body forces and surface forces at play in the FD of BPA. All these forces are proportional to some physical properties of the blood and/or the target, such as surface tension, viscosity, density, or wettability. It is therefore important to have accurate measurements of these physical properties. Also, while most BPA studies assume typical values for the physical properties, the blood of individuals has properties within a range of values. A cyclist competing for the *Tour de France* typically has more viscous blood, richer in Hematocrit [175, 176], than an average person. Therefore, studies could be performed to (1) assess the uncertainty involved in using typical physical properties; and (2) refine BPA methods to consider the physical properties of the specific protagonists identified in the bloodletting event. Precise knowledge of, for example, the viscosity and surface tension of the blood spilled at a crime scene might reduce the uncertainty associated with BPA.

A related and specific issue in BPA is that freshly drawn human blood potentially carries pathogens, so substitutes to human blood have been sought since early BPA studies [42] for the purpose of improving the safety of BPA research and teaching. As a result, research opportunities exist in BPA for the development or characterization of substitutes to fresh human blood, such as synthetic blood or animal blood.

Section 2 also describes an opportunity for the elaboration, publication and dissemination of regime maps that describe aspects of BPA within a dimensionless framework, with ratios of forces. Such maps could characterize the flight or breakup of drops (as in Figure 4), impact outcomes, and transformations during drying.

Section 3 reviews several aspects of the fluid dynamics of drop generation relevant to BPA. Importantly, high-speed measurements show that in several situations relevant to BPA the drops are not generated at a single point in space, but rather at the breakup location of an initial jet or liquid sheet, protruding from the area of origin of the blood spatter [13], during a cascade of events with specific temporal duration and spatial extension. This cascade of events needs to be

understood, modeled as simply as possible and considered for the reconstruction of ballistic trajectories. In that context, there is also an opportunity for models and experiments that link the kinematics of the bloodletting event to the size and speed of the generated drops. FD also offers several experimental tools to measure and simulate sprays, worthy of implementation in BPA research, as described in section 3.2.

While the breakup of jets and sheets has been widely investigated in FD, some drop generation mechanisms (gunshot and cast-off spatters) are specific to BPA and might benefit from systematic FD studies.

Section 4 reviews FD and BPA studies on the flight of drops. A full backward modeling of the ballistic trajectories of droplets is not yet available for the BPA practitioner. This possibly implies significant uncertainties on the determination of the area of origin. In that context, it would be useful to the BPA practitioner to have a simple method to discriminate between spatters that are suitable for the stringing method and the ones that call for ballistic trajectories. Also, the accurate reconstruction of curved trajectories (Figure 7, Figure 8) relies on the development of reliable methods to estimate the following variables explicitly: impact velocity, impact angle, and impacting drop size.

To the best of our knowledge, a framework is missing for the reconstruction of trajectories in non-quiescent air, such as gunshot spatters, injuries in windy conditions, or expirated spatters. Necessarily, that framework will involve solving the coupled problem of the airflow and the drop flight, a problem that is routinely solved in e.g. the design of fuel injectors. That example suggests that significant untapped expertise is available in the multiphase flow community, in terms of experimental, theoretical and numerical tools.

Section 5 reviews BPA and FD studies on the impact of drops, and describes the potential of computational fluid dynamics to study drop impact cases that are difficult to reproduce experimentally, involving, for example, the small drops travelling at high speed after a gunshot spatter. Related experiments are inherently difficult, in terms of measuring the ratios of drop

sizes over stain sizes, or of characterizing how a cloud of drops travels at velocities on the order of 100m/s.

The flight, impact and drying of blood drops is typically a non-isothermal process, since the blood is spilled at ~37°C and the air and target surface are at lower, room temperature. The resulting heat transfer modifies the physical properties of the drop significantly [70, 177], as described in section 4.2, with possible consequences on the amount of spreading during impact (see Table 4), on the stain formation, as has been shown for the related fields of e.g. maskless manufacturing [111]. Heat transfer analyses of drop impact can either be done analytically or via numerical simulations coupling heat transfer equations with the fluid dynamics equations.

There is also no general theory describing the influence of the target (e.g. roughness, permeability, wettability) on the spreading, fingering and splashing process. Specifically there is no simple model for dynamic wetting, although several approaches have been developed recently [24, 147, 178-180].

Section 6 reviews FD and BPA studies on the formation of stains. Little work has been done on the timing of drying processes, which possibly could tell about the chronology of the bloodletting events. As investigated by Herb MacDonell [181], the peripheral ring forming at the edge of bloodstains is more adherent than the center of the stain so that wiped-off bloodstains can be used to estimate the time between the staining and wipe-off event. Also, blood drops contain a specific ratio of liquid to solids, and three-dimensional measurements of stains are likely be correlated with the drop volume, a parameter relevant to the reconstruction of ballistic trajectories. To the best of our knowledge, another open problem would be to determine physical criteria for delamination.

A synthesis of the relations between FD and BPA is provided in Table 4c. This table shows in color the type of relationship between BPA concepts (rows, defined in Table 4a) and FD concepts (columns, defined in Table 4b), with colors indicating the type of relationship between the concepts. Table 4c also expresses the type of relation (non-existent, accidental, essential) and

includes more than 100 references. When available, key references from the literature are provided for individual cells of the table.

Stain size	Diameter of a circular stain; length and width for an elliptical stain.
Accompanying Drop	A small blood drop produced as a by-product of drop formation.
Altered Stain	A bloodstain with characteristics that indicate a physical change has occurred.
Angle of Impact	The acute angle (alpha), relative to the plane of a target, at which a blood drop strikes the target. At low impact angles a wave castoff (tiny splashed drop) is released from main drop in the direction of impact).
Area of Convergence; Directionality	The area containing the intersections generated by lines drawn through the long axes of individual stains that indicates in two dimensions (in a horizontal plane) the projected location of the blood source; The characteristic of a bloodstain that indicates the direction blood was moving at the time of deposition.
Area of Origin	The location in a 3-dimensional space from which the spatter originated.
Backspatter Pattern; Forward Spatter Pattern	A bloodstain pattern resulting from blood drops that traveled in the opposite direction of the external force applied; associated with an entrance wound created by a projectile; A bloodstain pattern resulting from blood drops that traveled in the same direction as the impact force.
Blood clot	A gelatinous mass formed by a complex mechanism involving red blood cells, fibrinogen, platelets, and other coagulations factors.
Bloodstain pattern	A grouping or distribution of bloodstains that indicates through regular or repetitive form, order, or arrangement the manner in which the pattern was deposited.
Bubble Ring; Expiration Pattern	An outline within a bloodstain resulting from air in the blood; A bloodstain pattern resulting from blood forced by airflow out of the nose, mouth, or a wound.
Cast-off Pattern; Cessation Cast-off Pattern	A bloodstain pattern resulting from blood drops released from an object due to its motion; A bloodstain pattern resulting from blood drops released from an object due to its rapid deceleration.
Directional Angle	The angle (gamma) between the long axis of a spatter stain and a defined reference line on the target.
Drip Stain; Drip Trail	A bloodstain resulting from a falling drop that formed due to gravity; A bloodstain pattern resulting from the movement of a source of drip stains between two points.
Edge Characteristic; Parent Stain; Satellite Stain; fingering; splash pattern	A physical feature of the periphery of a bloodstain; a bloodstain from which a satellite stain originated. A smaller bloodstain that originated during the formation of the parent stain as a result of blood impacting a surface; formation of spines at the edge of a stain; A bloodstain pattern resulting from a volume of liquid blood that falls or spills onto a surface.
Perimeter Stain	An altered stain that consists of the peripheral characteristics of the original stain.
Flow Pattern	A bloodstain pattern resulting from the movement of a volume of blood on a surface due to gravity or movement of the target.
Impact Pattern	A bloodstain pattern resulting from an object striking liquid blood.
Insect Stain	A bloodstain resulting from insect activity.
Mist Pattern	A bloodstain pattern resulting from blood reduced to a spray of micro-drops as a result of the force applied.
Serum Stain	The stain resulting from the liquid portion of blood (serum) that separates during coagulation.
Spatter Stain	A bloodstain resulting from a blood drop dispersed through the air due to an external force applied to a source of liquid blood.
Swipe pattern; transfer stain	A bloodstain pattern resulting from the transfer of blood from a blood-bearing surface onto another surface, with characteristics that indicate relative motion between the two surfaces; A bloodstain resulting from contact between a blood-bearing surface and another surface.
Drip Pattern	A bloodstain pattern resulting from a liquid that dripped into another liquid, at least one of which was blood.
Saturation Stain	A bloodstain resulting from the accumulation of liquid blood in an absorbent material.
Wipe Pattern	An altered bloodstain pattern resulting from an object moving through a preexisting wet bloodstain.
Projected Pattern	A bloodstain pattern resulting from the ejection of a volume of blood under pressure.
Deposit volume	The volume of a stain.

Table 4a: Definition of concepts relevant to BPA, adapted from the terminology working group of SWGSTAIN.

Rheology	Relationship between the rate of deformation and the mechanical stresses in a fluid.
Surface tension	Measure of the surface energy between two immiscible materials.
Substrate wettability	Affinity of a solid substrate with a pair of immiscible fluids along it.
Substrate roughness	Average amplitude and wavelength of height fluctuations on a surface.
Substrate elasticity	Ratio of the deformation of a solid surface to an applied normal force.
Dripping	Generation of a drop when gravity overcomes wetting forces.
Jet/sheet generation	Generation of a cylindrical (jet) or planar (sheet) volume of fluid, typically by inertial forces.
Jet/sheet breakup	Separation of the jet or sheet into unconnected liquid volumes such as drops or threads. Breakup is typically driven by instability formation and growth.
Trajectories	Motion of an object in a three-dimensional space, as a function of time.
Drag	Resistance to the flight of a drop, due to the inertia and friction of the surrounding fluid.
Pre-impact oscillations	Time-periodic shape changes during flight, i.e. between the generation and the impact.
Spreading	Deformation of a drop contacting a surface, without breakup in unconnected volumes.
Impact instabilities (fingers, hydraulic jump)	Changes of shape and velocity of the impacting liquid, growing with time at an exponential rate.
Bouncing/Rolling/sliding	During impact, a drop can rebound from the surface (bouncing). An oblique impact that results in motion parallel to the surface, without retention on the surface, is described as rolling or sliding.
Splashing	Deformation of a drop contacting a surface, involving breakup into unconnected liquid volumes.
Imbibition	Transport of a fluid in a porous material, driven by wetting forces and resisted by viscous forces.
Evaporation	Shrinkage of a drop by phase transformation of the liquid into vapor, in an endothermic process.
Phase change (coagulation)	Chemical transformation of the liquid blood into an interconnected network, with solid-type behavior.
Heat transfer	Transport of heat by conduction, convection or radiation.
Mixing	Transport of two species by random molecular motion (diffusion), or by the global motion of a fluid (convection).

Table 4b: Definition of concepts relevant to FD, from the authors.

Relations between Bloodstain Pattern Analysis (rows) and Fluid Dynamics (columns) **Unknown Relation** **No Relation** **Accidental Relation** **Essential Relation**		Property	Rheology Surface tension	Substrate wettability Substrate roughness	Substrate elasticity	Dripping	Jet/sheet generation; Jet/sheet breakup	Trajectories	Drag	Spreading	Impact instabilities (fingers, hydraulic jump); splashing	Bouncing/Rolling/sliding	Imbibition	Evaporation	Phase change (coagulation)	Heat transfer
Object investigated	**Inference**															
Stain size	*Impact conditions, weapon*		[107, 113 , 114, 131, 139, 182, 183]	[42, 113, 114, 126, 133, 134, 140, 184, 185]		[61, 62]	[5, 23, 35, 52, 58-60, 71, 72, 76, 78-81, 103-106]	[11, 41, 59, 107]	[5, 35-37, 186]	[13, 107, 112-114, 126-128, 187]	[126-128].	[154]	[42]		[170]	[70, 132, 177]
Accompanying Drop			[62, 63 , 64]			[61, 62, 66]					[142]					
Altered Stain	*aging, wipe*			[42, 188]									[188]	[174]	[160, 174]	
Angle of Impact	*area of origin*						[13 , 19, 68, 69 , 108, 109].	[5, 83, 89, 90, 91 , 92, 93, 97, 121, 122, 123 , 189]		[14, 41, 123]	[11, 14, 41, 94, 123, 125]					
Area of Convergence, Directionality							[13]	[5, 97]								
Area of Origin							[13, 19, 68, 69, 108, 109]	[9, 11, 89, 90, 95, 98, 121, 190]	[15, 35, 36, 42, 99, 186]		[14]					
Backspatter Pattern; Forward Spatter Pattern	*area of origin, weapon*						[48]	[5, 47, 110, 191]								
Blood Clot			[6, 162]												[160 , 162]	
Bloodstain pattern	*area of origin, weapon*		[13, 35, 76]					[13, 43, 82]	[36, 186]							
Bubble Ring; Expiration Pattern	*expiration pattern*		[81, 186]					[102]								
Cast-off Pattern; Cessation Cast-off Pattern	*motion, weapon, area of origin*							[5]								
Directional Angle	*Area of convergence*															
Drip Stain; Drip Trail	*height of origin; source-target relative motion*		[64 , 114, 126, 192]	[114, 142, 192]		[61, 62]		[114]	[5, 101, 114, 193]		[14]					
Edge Characteristic; Parent Stain; Satellite Stain; Fingering; Splash Pattern	*impact conditions: drop size, impact speed;*		[114, 126, 136, 142]	[4, 42, 89, 114, 119, 136, 142]	[25, 27, 128, 146]			[5, 11, 114, 118]			[14, 41, 42, 72, 76, 107, 114, 118, 128, 142, 144, 182, 194, 195]	[154]		[42, 166-170, 196]		[166, 170, 196]
Perimeter Stain	*time between drip and wipe-off,*		[155, 197, 198]	[155, 188]									[188]	[155, 163, 197, 198]		
Flow Pattern			[12, 162, 199]	[12, 162, 185, 199]						[185]					[12]	
Impact Pattern	*weapon, motion; directionality*		[78-80, 128]					[5]			[72, 128, 136]					
Insect Stain			[157, 200]													
Mist Pattern	*weapon, directionality*		[81, 154 , 186]				[58-60]	[47, 102]	[47, 102, 110]							
Spatter Stain									[201]			[126, 151-153]				
Swipe Pattern	*motion, weapon*		[173, 200]													
Drip Pattern	*height of origin*		[64, 65, 126, 128 , 137]			[61, 62]					[72] [136, 137]					
Saturation Stain	*side of cloth, staining mechanism (transfer, impact, contact)*		[21, 200, 202]	[21, 42, 120, 200, 202]									[21, 42, 120, 202]			
Wipe Pattern; Transfer stain	*motion, weapon*															
Projected Pattern			[23]					[47, 191]	[47, 191]							
Deposit Volume			[41 , 62]				[35, 76]							[156, 174]		

Table 4c: Connections between BPA (rows) and Fluid Dynamics concepts (columns). Note to the Editor: as proposed in our previous communication this table can be made available online if needed, as supplementary material.

8. Conclusion and epilogue

This manuscript has highlighted some key relationships between the disciplines of bloodstain pattern analysis (BPA) in forensics and that of fluid dynamics (FD) in the physical sciences. The body of knowledge related to drop generation, drop flight, drop impact, and stain formations has been presented as it is known in the BPA and FD communities. Table 1 and Table 2 summarize key physical properties and parameters relevant to BPA, with their typical values. Novel material has been proposed demonstrating the use of dimensionless numbers (Figure 3, Figure 4), assessing the importance of parabolic trajectories (Figure 7 and Figure 8). The intent of this work is to help build bridges between the BPA and FD communities, expanding and refining the many existing connections summarized in Table 4c. Also, in the context of the 2009 report of the US National Research Council advocating for stronger scientific foundations in BPA, several opportunities for joint research between BPA and FD have been mentioned.

Regarding the crime scene in Figure 1, the BPA analyst and coauthor C.M. proposed the following interpretation after a BPA analysis. The victim suffered multiple stab wounds and was left lying on the floor. During that time, blood pools on the kitchen floor (Area AE in Figure 1). Then, the victim stands up using the stove for support, probably causing with his arm the flow (AA) and transfer patterns (AB) on the stove. Standing still, blood drips causing the drip stain pattern (AD). Then the victim walks towards the living room, and is attacked again in the hallway**.** Several elliptical stains (B) on the hallway wall can be used to determine the area of origin of the resulting spatter. Can we expect joint future FD and BPA research to help refine this interpretation? Probably. Research on atomization mechanisms might clarify the causes of spatter B, be it for instance a beating or a stabbing. Research on ballistic reconstruction of trajectories might improve the determination of the area of origin of spatter B. Research on the drying of stains might help telling when the pool AE formed, and how much time elapsed before the victim stand up, forming the associated drip patterns AD.

REFERENCES

[1] T. Bevel and R. M. Gardner, *Bloodstain Pattern Analysis with an Introduction to Crime Scene Reconstruction*: CRC Press, Boca Raton, FL, USA, 2008.

[2] O. Darrigol, *Worlds of Flow: A History of Hydrodynamics from the Bernoullis to Prandtl*: Oxford University Press, 2005.

[3] "Strengthening Forensic Science in the United States: A Path Forward," Committee on Identifying the Needs of the Forensic Sciences Community, National Research Council2009.

[4] H. L. MacDonell, *Bloodstain Patterns*, 2nd. ed.: Laboratory of Forensic Sciences, Corning, NY USA, 2005.

[5] S. H. James, P. E. Kish, and T. P. Sutton, *Principles of Bloodstain Pattern Analysis: Theory and Practice*: CRC Press, 2005.

[6] I. Anadere, H. Chmiel, H. Hess, and G. B. Thurston, "Clinical blood rheology," *Biorheology*, vol. 16, pp. 171-178, 1979.

[7] B. A. J. Larkin, M. El-Sayed, D. A. C. Brownson, and C. E. Banks, "Crime scene investigation III: Exploring the effects of drugs of abuse and neurotransmitters on Bloodstain Pattern Analysis," *Analytical Methods*, vol. 4, pp. 721-729, 2012.

[8] M. J. Sweet, "Velocity Measurements of Projected Bloodstains from a Medium Velocity Impact Source," *Journal of Canadian Society of Forensic Science*, vol. 26, pp. 103-110, 1993.

[9] A. Pace, A. L. Carter, C. Moore, and B. Yamashita, "Another Treatment of Three-Dimensional Bloodstain Pattern Analysis," *International Association of Bloodstain Pattern Analysts News*, vol. 22, pp. 4-11, 2006.

[10] B. Brinkmann, B. Madea, and S. Rand, "Influencing factors of blood stain morphology," *Beitrage zur Gerichtlichen Medizin*, vol. VOL. 44, pp. 67-73, 1986.

[11] C. Knock and M. Davison, "Predicting the position of the source of blood stains for angled impacts," *J Forensic Sci*, vol. 52, pp. 1044-9, Sep 2007.

[12] J. Finsterer, C. Stöllberger, A. Hochfellner, A. Dossenbach-Glaninger, and P. Hopmeier, "Factors influencing the length of a blood trail," *Haemostasis*, vol. 29, pp. 353-354, 1999.

[13] N. Behrooz, L. Hulse-Smith, and S. Chandra, "An Evaluation of the Underlying Mechanisms of Bloodstain Pattern Analysis Error," *Journal of Forensic Sciences*, vol. 56, pp. 1136-1142, Sep 2011.

[14] C. D. Adam, "Fundamental studies of bloodstain formation and characteristics," *Forensic Sci Int*, Jan 5 2012.

[15] N. Behrooz, "Bloodstain Pattern Analysis for Determination of Point of Origin," B.S. Thesis, University of Toronto, Toronto, Canada, 2009.

[16] S. D. Gruttola, K. Boomsma, and D. Poulikakos, "Computational Simulation of a Non-Newtonian Model of the Blood Separation Process," *Artif Organs*, vol. 29, pp. 949-959, 2005.

[17] R. E. Wells, E. W. Merrill, and H. Gabelnick, "Shear Rate Dependence of Viscosity of Blood: Interaction of Red Cells and Plasma Proteins," *Transactions of the Society of Rheology*, vol. 6, pp. 19-24, 1962.

[18] L. Langstroth, "Blood viscosity: I. Conditions affecting the viscosity of blood after withdrawal from the body," *Journal of Experimental Medicine*, vol. 30, pp. 597-606, 1919.

[19] M. Raymond, E. Smith, and J. Liesegang, "The physical properties of blood – forensic considerations," *Science & Justice,* vol. 36, pp. 153-160, 1996.
[20] J. Rosina, E. Kvasnak, D. Suta, H. Kolarova, J. Malek, and L. Krajci, "Temperature dependence of blood surface tension," *Physiological Research,* vol. 56, pp. S93-S98, 2007.
[21] J. Bear, *Dynamics of Fluids in Porous Media*: Dover, 1988.
[22] S. Charm and G. Kurland, "Viscometry of human blood for shear rates of 0-100000 sec-1," *Nature,* vol. 206, pp. 617-618, 1965.
[23] J. Eggers and E. Villermaux, "Physics of liquid jets," *Reports on Progress in Physics,* vol. 71, 2008/// 2008.
[24] P. deGennes, F. Brochart-Wyart, and D. Quéré, *Capillarity and Wetting Phenomena: Drops, Bubbles, Pearls, Waves*: Springer, New York, 2003.
[25] R. E. Pepper, L. Courbin, and H. A. Stone, "Splashing on elastic membranes: The importance of early-time dynamics," *Physics of Fluids,* vol. 20, p. 082103, 2008.
[26] P. G. deGennes, "Wetting: Statics and Dynamics," *Rev. Mod. Phys.,* vol. 57, pp. 827-863, 1985.
[27] S. F. Kistler, "Hydrodynamics of Wetting," in *Wettability*, J. C. Berg, Ed., ed New York: Dekker, 1993.
[28] Z. Haiman, B. Kocsis, and K. Menou, "the population of viscosity- and gravitational wave-driven supermassive black hole binaries among luminous active galactic nuclei," *Astrophysical Journal,* vol. 700, pp. 1952-1969, Aug 2009.
[29] J. P. Shelby, J. White, K. Ganesan, P. K. Rathod, and D. T. Chiu, "A microfluidic model for single-cell capillary obstruction by Plasmodium falciparum -infected erythrocytes," *Proceedings of the National Academy of Sciences of the United States of America,* vol. 100, pp. 14618-14622, December 9, 2003 2003.
[30] R. H. Naylor, "Galileo and the Problem of Free Fall," *British Journal for the History of Science,* vol. 7, pp. 105-134, 1974.
[31] Galileo, *Discorsi e dimostrazioni matematiche, intorno à due nuove scienze, translated in 1963 as 'Dialogues concerning two new sciences' by H. Crew and A. de Salvio*: Dover, New York, 1638.
[32] S. Taneda, "Experimental investigation of the wake behind a sphere at low Reynolds numbers," *Journal of the Physical Society of Japan,* vol. 11, pp. 1104-1108, 1956.
[33] M. Ozgoren, E. Pinar, B. Sahin, and H. Akilli, "Comparison of flow structures in the downstream region of a cylinder and sphere," *International Journal heat and Fluid Flow,* vol. 32, pp. 1138-1146, 2011.
[34] E. J. Lavernia, E. M. Gutierrez, J. Szekely, and N. J. Grant, "A mathematical model for the liquid dynamic compaction process. Part 1: Heat flow in gas atomization," *Int. J . Rapid Solid.,* vol. 4, pp. 89-124, 1988.
[35] E. Villermaux, "Fragmentation," *Annual Review of Fluid Mechanics,* vol. 39, pp. 419-446, 2007.
[36] L. P. Hsiang and G. M. Faeth, "Drop deformation and breakup due to shock-wave and steady disturbances," *International Journal of Multiphase Flow,* vol. 21, pp. 545-560, Aug 1995.
[37] T. G. Theofanous, "Aerobreakup of Newtonian and Viscoelastic Liquids," in *Annual Review of Fluid Mechanics, Vol 43*. vol. 43, S. H. Davis and P. Moin, Eds., ed Palo Alto: Annual Reviews, 2011, pp. 661-690.

[38] L. I. Sedov, *Similarity and Dimensional Methods in Mechanics, Tenth Edition*: CRC Press, 1993.
[39] G. I. Barenblatt, *Scaling:Volume 34 of Cambridge Texts in Applied Mathematics*: Cambridge University Press, 2003.
[40] R. M. Gardner, "Defining the diameter of the smallest parent stain produced by a drip," *Journal of Forensic Identification,* vol. 56, pp. 210-221, 2006.
[41] P. A. Pizzola, S. Roth, and P. R. De Forest, "Blood droplet dynamics. I," *Journal of Forensic Sciences,* vol. 31, pp. 36-49, 1986.
[42] V. Balthazard, R. Piedelievre, H. Desoille, and L. Derobert, "Etude des gouttes de sang projete," in *XXIIe congres de medicine legale de langue francaise*, Paris, 1939.
[43] U. Buck, B. Kneubuehl, S. Näther, N. Albertini, L. Schmidt, and M. Thali, "3D bloodstain pattern analysis: ballistic reconstruction of the trajectories of blood drops and determination of the centres of origin of the bloodstains," *Forensic Sci Int,* vol. 206, pp. 22-8, Mar 20 2011.
[44] A. Armenti, Ed., *The physics of sports*. American Institute of Physics, 1992, p.^pp. Pages.
[45] A. Emes and C. Price. (1994.). *Blood In Slow Motion* [a video from the Metropolitain Police Forensic Science Laboratory].
[46] A. E. Donaldson, N. K. Walker, I. L. Lamont, S. J. Cordiner, and M. C. Taylor, "Characterising the dynamics of expirated bloodstain pattern formation using high-speed digital video imaging," *Int J Legal Med,* vol. 125, pp. 757-62, Nov 2011.
[47] J. O. Pex and C. H. Vaughan, "Observations of high velocity bloodspatter on adjacent objects," *Journal of Forensic Sciences,* vol. 32, pp. 1587-1594, 1987.
[48] M. C. Taylor, T. L. Laber, B. P. Epstein, D. S. Zamzow, and D. P. Baldwin, "The effect of firearm muzzle gases on the backspatter of blood," *Int J Legal Med,* vol. 125, pp. 617-28, Sep 2011.
[49] T. L. Laber, B. P. Epstein, and M. C. Taylor, "High speed digital video analysis of bloodstain pattern formation from common bloodletting mechanisms," *IABPA News,* pp. 4-12, 2008.
[50] T. L. Laber, B. P. Epstein, and M. C. Taylor. *High speed digital video analysis of bloodstain pattern formation from common bloodletting mechanisms, Bloodstain Pattern Analysis Video Collection, Midwest Forensic Center (Ames, IA)*. Available: www.mfrc.ameslab.gov
[51] E. MacCurdy, *The Notebooks of Leonardo da Vinci* vol. I & II: Reynal and Hitchcock, 1938.
[52] F. Savart, "Mémoire sur la constitution des veines liquides lancées par des orifices circulaires en mince paroi," *Ann. De Chim.*, vol. 53, pp. 337–386, 1833.
[53] A. M. Worthington, "A Second Paper on the Forms Assumed by Drops of Liquids Falling Vertically on a Horizontal Plate," *Proc. Roy. Soc. London,* vol. 25, pp. 498-503, 1877.
[54] A. M. Worthington, "On the Forms Assumed by Drops of Liquids Falling Vertically on a Horizontal Plate," *Proceedings of the Royal Society of London,* vol. 25, pp. 261-272, 1876.
[55] J. M. Kolinski, S. M. Rubinstein, S. Mandre, M. P. Brenner, D. A. Weitz, and L. Mahadevan, "Skating on a Film of Air: Drops Impacting on a Surface," *Physical Review Letters,* vol. 108, pp. 074503:1-5, Feb 2012.

[56] D. Attinger, Z. Zhao, and D. Poulikakos, "An Experimental Study of Molten Microdroplet Surface Deposition And Solidification: Transient Behavior and Wetting Angle Dynamics," *Journal of Heat Transfer,* vol. 122, pp. 544-556, 2000.
[57] A. Velten, E. Lawson, A. Bardagjy, M. Bawendi, and R. Raskar, "Slow art with a trillion frames per second camera," presented at the ACM SIGGRAPH 2011 Posters, Vancouver, British Columbia, Canada, 2011.
[58] W. D. Bachalo, "Experimental Methods in Multiphase Flows," *International Journal of Multiphase Flow,* vol. 20, pp. 261-295, Aug 1994.
[59] N. Damaschke, H. Nobach, T. I. Nonn, N. Semidetnov, and C. Tropea, "Multi-dimensional particle sizing techniques," *Experiments in Fluids,* vol. 39, pp. 336-350, 2005.
[60] C. Tropea, "Optical Particle Characterization in Flows," in *Annual Review of Fluid Mechanics*. vol. 43, S. H. Davis and P. Moin, Eds., ed Palo Alto: Annual Reviews, 2011, pp. 399-426.
[61] S. D. R. Wilson, "The slow dripping of a viscous fluid," *Journal of Fluid Mechanics,* vol. 190, pp. 561-570, May 1988.
[62] J. Eggers, "Drop formation - An overview," *ZAMM Zeitschrift fur Angewandte Mathematik und Mechanik,* vol. 85, pp. 400-410, 2005.
[63] H. M. Dong, W. W. Carr, and J. F. Morris, "An experimental study of drop-on-demand drop formation," *Physics of Fluids,* vol. 18, pp. 072102:1-16, 2006.
[64] X. D. Shi, M. P. Brenner, and S. R. Nagel, "A Cascade of Structure in a Drop Falling from a Faucet," *Science,* vol. 265, pp. 219-222, Jul 8 1994.
[65] O. E. Yildirim and O. A. Basaran, "Dynamics of formation and dripping of drops of deformation-rate-thinning and -thickening liquids from capillary tubes," *Journal of Non-Newtonian Fluid Mechanics,* vol. 136, pp. 17-37, Jun 2006.
[66] B. Ambravaneswaran, E. D. Wilkes, and O. A. Basaran, "Drop formation from a capillary tube: Comparison of one-dimensional and two-dimensional analyses and occurrence of satellite drops," *Physics of Fluids,* vol. 14, pp. 2606-2621, 2002.
[67] C. Clanet and J. C. Lasheras, "Transition from dripping to jetting," *Journal of Fluid Mechanics,* vol. 383, pp. 307-326, Mar 1999.
[68] C. D. Stow and M. G. Hadfield, "An Experimental Investigation of Fluid Flow Resulting from the Impact of a Water Drop with an Unyielding Dry Surface," *Proc. Roy. Soc. London A,* vol. 373, pp. 419-441, 1981.
[69] O. A. Basaran, "Nonlinear oscillations of viscous liquid drops," *Journal of Fluid Mechanics,* vol. 241, pp. 169-198, 1992.
[70] D. Attinger, S. Haferl, Z. Zhao, and D. Poulikakos, "Transport Phenomena in the Impact of a Molten Droplet on a Surface: Macroscopic Phenomenology and Microscopic Considerations. Part II: Heat Transfer and Solidification.," *Annual Review of Heat Transfer,* vol. XI, pp. 65-143, 2000.
[71] A. H. Lefebvre, *Atomization and Sprays*. New York: Hemisphere, 1989.
[72] I. V. Roisman, K. Horvat, and C. Tropea, "Spray impact: Rim transverse instability initiating fingering and splash, and description of a secondary spray," *Physics of Fluids,* vol. 18, Oct 2006.
[73] M. Taylor. *Cough through bloodied lips {High Speed Visualization}*. Available: https://www.mfrc.ameslab.gov/files/Bloodletting%20Mechanism%20Videos/15Ac3%20Cough%20through%20bloodied%20lips.avi

[74] D. F. Rutland and G. J. Jameson, "A non-linear effect in the capillary instability of liquid jets," *Journal of Fluid Mechanics,* vol. 46, pp. 267-271, 1971.
[75] M. V. Dyke, *An Album of Fluid Motion*: The Parabolic Press, Stanford California, 1982.
[76] E. Villermaux and B. Bossa, "Drop fragmentation on impact," *Journal of Fluid Mechanics,* vol. 668, pp. 412-435, 2011.
[77] W. A. Sirignano and C. Mehring, "Review of theory of distortion and disintegration of liquid streams," *Progress in Energy and Combustion Science 26 (2000) 609–655,* vol. 26, pp. 609–655, 2000.
[78] A. Korobkin, "Shallow-water impact problems," *Journal of Engineering Mathematics,* vol. 35, pp. 233-250, Feb 1999.
[79] A. A. Korobkin, "Asymptotic Theory of Liquid-Solid Impact," *Phil. Trans. R. Soc. Lond. A,* vol. 355, pp. 507--522, 1997.
[80] A. A. Korobkin and V. V. Pukhnachov, "Initial stage of water impact," *Annual Review of Fluid Mechanics,* vol. 20, pp. 159-185, 1988.
[81] S. P. Lin and R. D. Reitz, "Drop and spray formation from a liquid jet," *Annual Review of Fluid Mechanics,* vol. 30, pp. 85-105, 1998.
[82] K. Walcher, *Gerichtlich-medizinische und kriminalistische Blutuntersuchung ein Leitfaden fuer Studierende, Aerzte und Kriminalisten; translation of pages 15-33 concerning "The shape of blood stains"*. Berlin: Springer, 1939.
[83] P. L. Kirk, *Affidavit Regarding State of Ohio V. Samual Sheppard*: Court of Common Pleas, Criminal Branch, No. 64571, 26 April 1955.
[84] M. B. Illes, A. L. Carter, P. L. Laturnus, and A. B. Yamashita, "Use of the BackTrack computer program for bloodstain pattern analysis of stains from downward-moving drops," *Journal of the Canadian Society of Forensic Science,* vol. 38, pp. 213-217, 2005.
[85] A. L. Carter, "The Directional Analysis of Bloodstain Patterns: Theory and Experimental Validation," *Journal of the Canadian Society of Forensic Science,* vol. 34, pp. 173-173, 2001.
[86] R. Kanable, "BackTrack Going Forward," *Law Enforcement Technology,* pp. 40-45, 2006.
[87] A. L. Carter, "Validation of the BackTrackTM Suite of Programs for Bloodstain Pattern Analysis," *Journal of Forensic Identification,* vol. 56, pp. 242-254, 2006.
[88] A. L. Carter, M. Illes, K. Maloney, A. B. Yamashita, B. Allen, B. Brown, L. Davidson, G. Ellis, J. Gallant, A. Gradkowski, J. Hignell, S. Jory, P. L. Laturnus, C. C. Moore, R. Pembroke, A. Richard, R. Spenard, and C. Stewart, "Further Validation of the BackTrack(TM) Computer Program for Bloodstain Pattern Analysis: Precision and Accuracy," *International Association of Bloodstain Pattern Analysts News,* vol. 21, pp. 15-22, 2005.
[89] J. K. Wells, "Investigation of Factors Affecting the Region of Origin Estimate in Bloodstain Pattern Analysis," MS Thesis, University of Canterbury, 2006.
[90] A. L. Carter, "Bloodstain Pattern Analysis with a Computer," in *Scientific and Legal Applications of Bloodstain Pattern Interpretation,* ed: CRC Press, Boca Raton, FL, USA, 1998, pp. 17-28.
[91] M. Illes and M. Boué, "Investigation of a Model for Stain Selection in Bloodstain Pattern Analysis," *Can. Soc. Forensic Sci. J.,* vol. 44, pp. 1-12, 2011.

[92] M. B. Illes, "Investigation of a model for stain selection and a robust estimation for area of origin in bloodstain pattern analysis," MS Thesis, Trent University, Ontario, Canada, 2011.
[93] J. Wells, "Investigation of factors affecting the region of origin estimates in bloodstain pattern analysis [Master's Thesis]. ," Canterbury (New Zealand): University of Canterbury, 2006.
[94] H. Templeman, "Errors in Blood Droplet Impact Angle Reconstruction Using a Protractor," *Journal of Forensic Identification,* vol. 40, pp. 15-24, 1990.
[95] W. F. Rowe, "Errors in the determination of the point of origin of bloodstains," *Forensic Science International,* vol. 161, pp. 47-51, Aug 2006.
[96] C. Connolly, M. Illes, and J. Fraser, "Affect of Impact Angle Variations on Area of Origin Determination in Bloodstain Pattern Analysis," *Forensic Science International,* vol. 223, pp. 233-240, 2012.
[97] K. G. de Bruin, R. D. Stoel, and J. C. M. Limborgh, "Improving the Point of Origin Determination in Bloodstain Pattern Analysis," *Journal of Forensic Sciences,* vol. 56, pp. 1476-1482, 2011.
[98] P. A. Pizzola, J. M. Buszka, N. Marin, N. D. K. Petraco, and P. R. De Forest, "Commentary on "3D bloodstain pattern analysis: Ballistic reconstruction of the trajectories of blood drops and determination of the centres of origin of the bloodstains" by Buck et al. [Forensic Sci. Int. 206 (2011) 22-28]," *Forensic Sci Int,* vol. 220, pp. e39-e40, 2012.
[99] B. T. Cecchetto, "Nonlinear Blood Pattern Reconstruction," MS thesis, The University of British Columbia, Vancouver, Canada, 2010.
[100] C. R. Varney and F. Gittes, "Locating the source of projectile fluid droplets," *American Journal of Physics,* vol. 79, pp. 838-842, 2011.
[101] W. D. Flower, "The terminal velocity of drops," *Proceedings of the Physical Society,* vol. 40, pp. 167-176, 1927.
[102] D. Denison, A. Porter, M. Mills, and R. C. Schroter, "Forensic implications of respiratory derived blood spatter distributions," *Forensic Sci Int,* vol. 204, pp. 144-55, Jan 30 2011.
[103] Y. Hardalupas and C. H. Liu, "Implications of the Gaussian intensity distribution of laser beams on the performance of the phase Doppler technique, sizing uncertainties," *Progress in Energy and Combustion Science,* vol. 23, pp. 41-63, 1997.
[104] I. Nagao, K. Matsumoto, and H. Tanaka, "Characteristics of dimethylsulfide, ozone, aerosols, and cloud condensation nuclei in air masses over the northwestern Pacific Ocean," *Journal of Geophysical Research-Atmospheres,* vol. 104, pp. 11675-11693, May 1999.
[105] J. U. Otaigbe, M. D. Barnes, K. Fukui, B. G. Sumpter, and D. W. Noid, "Generation, characterization, and modeling of polymer micro- and nano-particles," *Polymer Physics and Engineering,* vol. 154, pp. 1-86, 2001.
[106] C. Lacour, D. Durox, S. Ducruix, and M. Massot, "Interaction of a polydisperse spray with vortices," *Experiments in Fluids,* vol. 51, pp. 295-311, Aug 2011.
[107] L. Hulse-Smith and M. Illes, "A blind trial evaluation of a crime scene methodology for deducing impact velocity and droplet size from circular bloodstains," *J Forensic Sci,* vol. 52, pp. 65-9, Jan 2007.

[108] M. A. Raymond, E. R. Smith, and J. Liesegang, "Oscillating blood droplets - implications for crime scene reconstruction," *Science and Justice - Journal of the Forensic Science Society,* vol. 36, pp. 161-171, 1996.
[109] M. Raymond, J. Liesegang, and E. Smith, "High speed cinematography of blood droplet deformation in flight—implications for crime scene reconstruction.," in *Advances in forensic sciences— Proceedings of the 13th Meeting of the International Association of Forensic Sciences*, Duesseldorf, Germany, 1993, pp. 200–207.
[110] D. J. Carlson and R. F. Hoglund, "Particle Drag and Heat Transfer in Rocket Nozzles," *Aiaa Journal,* vol. 2, pp. 1980-1984, 1964.
[111] D. Poulikakos and J. Waldvogel, "Heat Transfer and Fluid Dynamics in the Process of Spray Deposition," *Adv. Heat Transfer,* vol. 28, pp. 1-74, 1996.
[112] O. G. Engel, "Waterdrop Collisions with Solid Surfaces," *J. Res. Nat. Bur. Stand.,* vol. 54, pp. 281-298, 1955.
[113] M. Pasandideh-Fard, Y. M. Qiao, S. Chandra, and J. Mostaghimi, "Capillary Effects during Droplet Impact on a Solid Surface," *Phys. Fluids,* vol. 8, pp. 650-659, 1996.
[114] L. Hulse-Smith, N. Z. Mehdizadeh, and S. Chandra, "Deducing drop size and impact velocity from circular bloodstains," *Journal of Forensic Sciences,* vol. 50, pp. 54-63, 2005.
[115] , F. Girard, and V. Morin, "An energy balance approach of the dynamics of drop impact on a solid surface," *Physics of Fluids,* vol. 19, pp. 012101:1-17, 2007.
[116] H. B. Humberstone, "Charlie Chan at the race track," ed: 20th Century Fox, 1936.
[117] H. Marmanis and S. T. Thoroddsen, "Scaling of the fingering pattern of an impacting drop," *Physics of Fluids,* vol. 8, pp. 1344-1344, 1996.
[118] N. Z. Mehdizadeh, S. Chandra, and J. Mostaghimi, "Formation of fingers around the edges of a drop hitting a metal plate with high velocity," *Journal of Fluid Mechanics,* vol. 510, pp. 353-373, Jul 2004.
[119] H. L. MacDonell and L. F. Bialousz, "Flight characteristics and stain patterns of human blood," Report to the National Institute of Law Enforcement and Criminal Justice, US Dept of Justice, Law Enforcement Assistance Administration, Washington, DC1971.
[120] P. L. Kirk, *Crime Investigation:physical evidence and the police laboratory*: Interscience Publishers, 1953.
[121] C. Willis, A. K. Piranian, J. R. Donaggio, R. J. Barnett, and W. F. Rowe, "Errors in the estimation of the distance of fall and angles of impact blood drops," *Forensic Science International,* vol. 123, pp. 1-4, Nov 2001.
[122] C. Rizer, "Police Mathematics," ed: Charles C. Thomas, Springfield, IL, 1955, pp. 72-73.
[123] P. A. Pizzola, S. Roth, and P. R. De Forest, "Blood droplet dynamics. II," *Journal of Forensic Sciences,* vol. 31, pp. 50-64, 1986.
[124] C. Knock and M. Davison, "Predicting the Position of the Source of Blood Stains for Angled Impacts," *Journal of Forensic Sciences,* vol. 52, pp. 1044-1049, 2007.
[125] J. C. Bird, S. S. H. Tsai, and H. A. Stone, "Inclined to splash: triggering and inhibiting a splash with tangential velocity," *New Journal of Physics,* vol. 11, pp. 063017:1-11, 2009.
[126] A. L. Yarin, "Drop impact dynamics: splashing, spreading, receding, bouncing," *Annual Review of Fluid Mechanics,* vol. 38, pp. 159-159, 2005.
[127] S. Haferl, Z. Zhao, J. Giannakouros, D. Attinger, and D. Poulikakos, "Transport Phenomena in the Impact of a Molten Droplet on a Surface: Macroscopic Phenomenology and Microscopic Considerations. Part I: Fluid Dynamics," in *Annual*

Review of Heat Transfer. vol. XI, C. L. Tien, Ed., ed: Begell House, NY, 2000, pp. 145-205.
[128] M. Rein, "Phenomena of Liquid Drop Impact on Solid and Liquid Surfaces," *Fluid Dynamics Research,* vol. 12, pp. 61-93, 1993.
[129] F. H. Harlow and J. P. Shannon, "The Splash of a Liquid Drop," *J. Appl. Phys.,* vol. 38, pp. 3855-3866, 1967.
[130] M. Bertagnolli, M. Marchese, G. Jacucci, I. S. Doltsinis, and S. Noelting, "Thermomechanical Simulation of the Splashing of Ceramic Droplets on a Rigid Substrate," *J. Comp. Phys.,* vol. 133, pp. 205-221, 1997.
[131] J. Fukai, Y. Shiba, T. Yamamoto, O. Miyatake, D. Poulikakos, C. M. Megaridis, and Z. Zhao, "Wetting Effects on the Spreading of a Liquid Droplet Colliding with a Flat Surface: Experiment and Modeling," *Physics of Fluids,* vol. 7, pp. 236-247, 1995.
[132] Z. Zhao, D. Poulikakos, and J. Fukai, "Heat Transfer and Fluid Dynamics during the Collision of a Liquid Droplet on a Substrate: II-Experiments," *International Journal Heat Mass transfer,* vol. 39, pp. 2791-2802, 1996.
[133] T. D. Blake and J. DeConinck, "The influence of solid-liquid interactions on dynamic wetting," *Advances in Colloid and Interface Science,* vol. 66, p. 21, 2002.
[134] R. Bhardwaj and D. Attinger, "Non-isothermal wetting during impact of millimeter size water drop on a flat substrate: numerical investigation and comparison with high speed visualization experiments," *International Journal of Heat and Fluid Flow,* vol. 29, pp. 1422-1435, 2008.
[135] D. Attinger and D. Poulikakos, "Melting and Resolidification of a Substrate caused by Molten Microdroplet Impact," *Journal of Heat Transfer,* vol. 123, pp. 1110-1122, 2001.
[136] C. Mundo, M. Sommerfeld, and C. Tropea, "Droplet-Wall Collisions: Experimental Studies of the Deformation and Breakup Process," *Int. J. Multiphase Flow,* vol. 21, pp. 151-173, 1995.
[137] R. Rioboo, C. Bauthier, J. Conti, M. Voué, and J. De Coninck, "Experimental investigation of splash and crown formation during single drop impact on wetted surfaces," *Experiments in Fluids,* vol. 35, pp. 648-652, 2003.
[138] P. Roura and J. Fort, "Comment on "Effects of the Surface Roughness on Sliding Angles of Water Droplets on Superhydrophobic Surfaces"," *Langmuir,* vol. 18, pp. 566-569, 2002.
[139] T. Mao, D. C. S. Kuhn, and H. Tran, "Spread and rebound of liquid droplets upon impact on flat surfaces," *Aiche Journal,* vol. 43, pp. 2169-2179, 1997.
[140] S. Chandra and C. T. Avedisian, "On the Collision of a Droplet with a Solid Surface," *Proc. R. Soc. Lond. A,* vol. 432, pp. 13-41, 1991.
[141] C. Josserand, L. Lemoyne, R. Troeger, and S. Zaleski, "Droplet Impact on a Dry Surface: Triggering the Splash with a Small Obstacle," *Journal of Fluid Mechanics,* vol. 524, pp. 47-56, 2005.
[142] S. Mandre and M. P. Brenner, "The mechanism of a splash on a dry solid surface," *Journal of Fluid Mechanics,* vol. 690, pp. 148-172, Jan 2012.
[143] L. Xu, W. W. Zhang, and S. R. Nagel, "Drop splashing on a dry smooth surface," *Physical Review Letters,* vol. 94, pp. 184505:1-4, May 2005.
[144] R. E. Ford and C. G. L. Furmidge, "Impact and spreading of spray drops on foliar surfaces," *Wetting,* vol. 25, pp. 417-432, 1967.

[145] M. B. Lesser, "Analytic Solutions of Liquid-Drop Impact Problems," *Proc. Roy. Soc. London A,* vol. 377, pp. 289-308, 1981.
[146] J. E. Field, J. P. Dear, and J. E. Ogren, "The Effects of Target Compliance on Liquid Drop Impact," *J. Appl. Phys.*, vol. 62, pp. 533-540, 1988.
[147] A. Joshi and Y. Sun, "Wetting dynamics and particle deposition for an evaporating colloidal drop: A lattice Boltzmann study," *Physical Review E,* vol. 82, 2010.
[148] I. S. Bayer and C. M. Megaridis, "Contact angle dynamics in droplets impacting on flat surfaces with different wetting characteristics," *Journal of Fluid Mechanics,* vol. 558, pp. 415-449, Jul 10 2006.
[149] Š. Šikalo, C. Tropea, and E. N. Ganic, "Dynamic wetting angle of a spreading droplet," *EXPERIMENTAL THERMAL AND FLUID SCIENCE,* vol. 29, pp. 795-802, 2005.
[150] D. Attinger, "An Investigation of Molten Microdroplet Surface Deposition: Transient Behavior, Wetting Angle Dynamics and Substrate Melting Phenomenon; Ph.D. thesis," Ph.D. Thesis, Department of Mechanical Engineering, Eidgenoessische Technische Hochschule (ETH), Zurich, 2001.
[151] L. Chen and Z. Li, "Bouncing droplets on nonsuperhydrophobic surfaces," *Physical Review E,* vol. 82, 2010.
[152] D. Caviezel, C. Narayanan, and D. Lakehal, "Adherence and bouncing of liquid droplets impacting on dry surfaces," *Microfluidics and Nanofluidics,* vol. 5, pp. 469-478, Oct 2008.
[153] D. Bartolo, F. Bouamrirene, E. Verneuil, A. Buguin, P. Silberzan, and S. Moulinet, "Bouncing or sticky droplets: Impalement transitions on superhydrophobic micropatterned surfaces," *Europhysics Letters,* vol. 74, pp. 299-305, 2006/// 2006.
[154] C. G. L. Furmidge, "Studies at phase interfaces. I. The sliding of liquid drops on solid surfaces and a theory for spray retention," *Journal of Colloid Science,* vol. 17, pp. 309-324, 1962.
[155] R. D. Deegan, O. Bakajin, T. F. Dupont, G. Huber, S. R. Nagel, and T. A. Witten, "Capillary flow as the cause of ring stains from dried liquid drops," *Nature,* vol. 389, pp. 827-829, 1997.
[156] D. Brutin, B. Sobac, B. Loquet, and J. Sampol, "Pattern formation in drying drops of blood," *Journal of Fluid Mechanics,* vol. 667, pp. 85-95, 2011.
[157] R. E. Brown, R. I. Hawkes, M. A. Parker, and J. H. Byrd, "Entomological Alteration of Bloodstain Evidence," in *Entomological Alteration of Bloodstain Evidence: The Utility of Arthropods in Legal Investigations,* ed Boca Raton, FL: CRC Press, 2001, pp. 353-378.
[158] A. Becue, S. Moret, C. Champod, and P. Margot, "Use of quantum dots in aqueous solution to detect blood fingermarks on non-porous surfaces," *Forensic Sci Int,* vol. 191, pp. 36-41, Oct 30 2009.
[159] S. Boyd, M. F. Bertino, and S. J. Seashols, "Raman spectroscopy of blood samples for forensic applications," *Forensic Sci Int,* vol. 208, pp. 124-8, May 20 2011.
[160] R. H. Bremmer, K. G. de Bruin, M. J. van Gemert, T. G. van Leeuwen, and M. C. Aalders, "Forensic quest for age determination of bloodstains," *Forensic Sci Int,* vol. 216, pp. 1-11, Mar 10 2012.
[161] D. Brutin, B. Sobac, and C. Nicloux, "Influence of Substrate Nature on the Evaporation of a Sessile Drop of Blood," *Journal of Heat Transfer-Transactions of the Asme,* vol. 134, Jun 2012.
[162] M. Kaibara, "Rheology of blood coagulation," *Biorheology,* vol. 33, pp. 101-117, 1996.

[163] W. D. Ristenpart, P. G. Kim, C. Domingues, J. Wan, and H. A. Stone, "Influence of Substrate Conductivity on Circulation Reversal in Evaporating Drops," *Physical Review Letters,* vol. 99, pp. 234502:1-4, 2007.
[164] R. Bhardwaj, X. Fang, P. Somasundaran, and D. Attinger, "Self-assembly of colloidal particles from evaporating droplets: role of the pH and proposition of a phase diagram," *Langmuir,* vol. 26, pp. 7833-7842, 2010.
[165] H. Hu and R. G. Larson, "Evaporation of a sessile droplet on a substrate," *Journal of Physical Chemistry B,* vol. 106, pp. 1334-1344, 2002.
[166] H. Hu and R. G. Larson, "Analysis of Microfluid flow in an Evaporating sessile droplet," *Langmuir,* vol. 21, pp. 3963-3971, 2005.
[167] B. J. Fischer, "Particle convection in an evaporating droplet," *Langmuir,* vol. 18, pp. 60-67, 2002.
[168] H. Hu and R. G. Larson, "Marangoni Effect Reversed Coffee-Ring Depositions," *Journal of Physical Chemistry B,* vol. 110, pp. 7090-7094, 2006.
[169] E. Widjaja and M. T. Harris, "Particle deposition study during sessile drop evaporation," *AIChe journal,* vol. 54, pp. 2250-2260, 2008.
[170] R. Bhardwaj, X. Fang, and D. Attinger, "Pattern formation during the evaporation of a colloidal nanoliter drop: a numerical and experimental study," *New Journal of Physics,* vol. 11, pp. 075020:1-33, 2009.
[171] E. W. Washburn, "The dynamics of capillary flow," *Physical Review,* vol. 17, pp. 273-283, 1921.
[172] J. Xiao, H. A. Stone, and D. Attinger, "Source-like solution for radial imbibition into a homogeneous semi-infinite porous medium," *Langmuir,* vol. 28, pp. 4208-12, Mar 6 2012.
[173] B. Simoncic and V. Rozman, "Wettability of cotton fabric by aqueous solutions of surfactants with different structures," *Colloids and Surfaces A: Physicochemical and Engineering Aspects,* vol. 292, pp. 236-245, 2007.
[174] C. Allain and L. Limat, "Regular patterns of cracks formed by directional drying of a colloidal suspension," *physical Review Letters,* vol. 74, pp. 2981-2984, 1995.
[175] N. Robinson, L. Schattenberg, M. Zorzoli, P. Mangin, and M. Saugy, "Haematological analysis conducted at the departure of the Tour de France 2001," *International Journal of Sports Medicine,* vol. 26, pp. 200-207, Apr 2005.
[176] J. S. Mørkeberg, B. Belhage, and R. Damsgaard, "Changes in Blood Values in Elite Cyclist," *International Journal of Sports Medicine,* vol. 30, pp. 130-138, Feb 2009.
[177] R. Bhardwaj, J. P. Longtin, and D. Attinger, "Interfacial temperature measurements, high-speed visualization and finite-element simulations of droplet impact and evaporation on a solid surface," *International Journal Heat Mass transfer,* vol. 53, pp. 3733-3744, 2010.
[178] T. D. Blake, R. A. Dobson, and K. J. Ruschak, "Wetting at high capillary numbers," *J Colloid Interface Sci,* vol. 279, pp. 198-205, Nov 1 2004.
[179] S. R. Ranabothu, C. Karnezis, and L. L. Dai, "Dynamic wetting: hydrodynamic or molecular-kinetic?," *J Colloid Interface Sci,* vol. 288, pp. 213-21, Aug 1 2005.
[180] J. B. Freund, "The atomic detail of a wetting/de-wetting flow," *Physics of Fluids,* vol. 15, pp. L33-L36, 2003.
[181] H. L. MacDonell, "Age of a bloodstain before it was wiped, CD describing research work of F. Trassati," in *meeting with D. Attinger*, ed, january 2010.

[182] S. Sikalo and E. N. Ganič, "Phenomena of droplet-surface interactions," *Experimental Thermal and Fluid Science,* vol. 31, pp. 97-110, 2006.
[183] M. Pasandideh-Fard, S. Chandra, and J. Mostaghimi, "A three-dimensional model of droplet impact and solidification," *International Journal of Heat and Mass Transfer,* vol. 45, pp. 2229-2242, 2002.
[184] R. Rioboo, M. Marengo, and C. Tropea, "Time evolution of liquid drop impact onto solid, dry surfaces," *Experiments in Fluids,* vol. 33, pp. 112-124, 2002.
[185] M. Miwa, A. Nakajima, A. Fujishima, K. Hashimoto, and T. Watanabe, "Effects of the Surface Roughness on Sliding Angles of Water Droplets on Superhydrophobic Surfaces," *Langmuir,* vol. 16, pp. 5754-5760, 2000.
[186] B. F. Gelfand, "Droplet breakup phenomena in flows with velocity lag," *Prog. Energy Combustion Science,* vol. 22, pp. 201-265, 1996.
[187] L. Cheng, "Dynamic Spreading of Drops Impacting onto a Solid Surface," *Ind. Eng. Chem.,* vol. 16, pp. 192-197, 1977.
[188] C. Corby, C. Hauke, B. Gestring, and L. Quarino, "Preliminary Study Analyzing the Halo Effect: Factors Involved in Sequencing the Deposition of Overlapping Bloodstains Caused by Wipe Patterns and Blood Droplets," *Investigative Sciences Journal,* vol. 4, 2012.
[189] F. Chafe, "Determination of Impact Angle Using Mathematical Properties of the Ellipse," *International Association of Bloodstain Pattern Analysts News,* vol. 19, pp. 5-9, 2003.
[190] H. L. MacDonell, "No More Strings, No More Computers, just simple Mathematics, that's all it takes," *International Association of Bloodstain Pattern Analysts News,* vol. 12, pp. 10-10, 1996.
[191] B. G. Stephens and T. B. Allen, "Back spatter of blood from gunshot wounds. Observations and experimental simulation," *Journal of Forensic Sciences,* vol. 28, pp. 437-439, 1983.
[192] H. Fujimoto, Y. Shiotani, A. Tong, T. Hama, and H. Takuda, "Three-dimensional numerical analysis of the deformation behavior of droplets impinging onto a solid substrate," *International Journal of Multiphase Flow,* vol. 33, pp. 317-332, 2007.
[193] K. V. Beard and H. R. Pruppacher, "A Determination of the Terminal Velocity and Drag of Small Water Drops by Means of a Wind Tunnel," *Journal of the Atmospheric Sciences,* vol. 26, pp. 1066-1072, 1969.
[194] S. T. Thoroddsen and J. Sakakibara, "Evolution of the Fingering Pattern of an Impacting Drop," *Phys. Fluids,* vol. 10, pp. 1359-1374, 1998.
[195] A. L. Gonor and V. Y. Yakovlev, "Dynamics of the impact of a drop on a solid surface," *Fluid Dynamics,* vol. 13, pp. 25-31, 1978.
[196] H. Hu and R. G. Larson, "Evaporation of a sessile droplet on a substrate," *Journal of Physical Chemistry B,* vol. 106, pp. 1334-1344, 2002.
[197] R. Bhardwaj, X. Fang, P. Somasundaran, and D. Attinger, "Self-assembly of colloidal particles from evaporating droplets: role of DLVO interactions and proposition of a phase diagram," *Langmuir,* vol. 26, pp. 7833-42, Jun 1 2010.
[198] G. Berteloot, C. T. Pham, A. Daerr, F. Lequeux, and L. Limat, "Evaporation-induced flow near a contact line: Consequences on coating and contact angle," *EPL (Europhysics Letters),* vol. 83, pp. 14003:1-5, 2008.
[199] Y. Pomeau and E. Villermaux, "Two hundred years of capillarity research," *Physics Today,* vol. 59, pp. 39-44, Mar 2006.

[200] C. M. Reed and N. Wilson, "The fundamentals of absorbency of fibres, textile structures and polymers. I. The rate of rise of a liquid in glass capillaries," *Journal of physics D: Applied physics*, vol. 26, pp. 1378-1378, 1993.
[201] E. M. F. D'Albe and M. S. Hidayetulla, "The break-up of large water drops falling at terminal velocity in free air," *Quarterly Journal of the Royal Meteorological Society*, vol. 81, pp. 610-613, 1955.
[202] B. Simončič and V. Rozman, "Wettability of cotton fabric by aqueous solutions of surfactants with different structures," *Colloids and Surfaces A: Physicochemical and Engineering Aspects*, vol. 292, pp. 236-245, 2007.

Appendix A: Calculations of the various integrals presented in section 2.2.1

In this appendix we provide exact expressions of the integrals defined in section 2.2.1. Note that the trajectories are along a vertical z-axis oriented upwards, with the target at *z=0* and the release of the drop at a height *z=h*.

In equation (6), the ratio Δ of the work of the drag force W_D over the initial kinetic energy E_{k0} can be calculated numerically with the following integral

$$\Delta = W_D/E_{k0} = \frac{\int_h^0 F_D dz}{\frac{1}{2} m v_0^2} = \frac{\int_h^0 \frac{1}{2}\rho_a C_D A_d \vec{v} v \, dz}{\frac{1}{2} m v_0^2} = -\frac{3\rho_a \int_h^0 C_D \left(\frac{dh}{dt}\right)^2 dz}{2 d_0 \rho_L v_0^2} \quad (12),$$

where *h* is the height of the fall, and the drag force F_D is a function of the local velocity, as per eqts (2) and (3). The term left in the integral of eq. (12) needs to be calculated by numerical integration of the trajectories.

In equation (5), the ratio of the gravity work W_g over the initial kinetic energy E_{k0} can be calculated from the initial conditions

$$G = \frac{\int_h^0 -mg\, dz}{\frac{1}{2} m v_0^2} = \frac{2gh}{v_0^2} \quad (13).$$

In equation (7), the ratio $\Gamma = mg/F_D$ of the weight over the drag force can be expressed and simplified as

$$\Gamma = \frac{mg}{F_D} = \frac{4\rho_L d_0 g}{3 C_D \rho_a v_0^2} \quad (14).$$

Appendix B: How to use of impact velocity plot in section 2.2.1, Figure 4

Steps to determine the impact velocity from known initial velocity v_0 and initial diameter d_0, using Figure 4:

1. Input d_0 on horizontal axis.
2. Move vertically until crossing the violet curve: the terminal velocity $v_{terminal}$ is found on the violet vertical axis, right, at the same vertical level.
3. Identify ratio $v_0/v_{terminal}$ of the initial velocity over terminal velocity on the vertical axis, left.
4. The ratio of impact velocity over terminal velocity is determined by the contour value at the intersection of the vertical line passing by d_0 and the horizontal line passing by $v_0/v_{terminal}$.

Example (shown by capital letters in Figure 4)

Step\Example	A	B	C
v_0	3.5 m/s	50 m/s	0 m/s
Step 1: d_0	0.2 mm	4 mm	4 mm
Step 2: $v_{terminal}$	≈ 0.7 m/s	≈ 10.3 m/s	≈ 10.3 m/s
Step 3: $v_0/v_{terminal}$	≈ 5	No value, as drop breaks up into smaller drops	0
Step 5: $v_{impact}/v_{terminal}$	≈ 1.0		≈ 0.4
Step 5: v_{impact}	≈ 0.7 m/s		≈ 4.1 m/s